Journal of MATERIALS RESEARCH

Invited Paper
DOI:10.1557/s43578-022-00591-5

Engineered 2D materials for optical bioimaging and path toward therapy and tissue engineering

Jeewan C. Ranasinghe[1], Arpit Jain[2], Wenjing Wu[1], Kunyan Zhang[1], Ziyang Wang[1], Shengxi Huang[1,a)]

[1] Department of Electrical Engineering, The Pennsylvania State University, University Park, PA 16802, USA
[2] Department of Materials Science and Engineering, The Pennsylvania State University, University Park, PA 16802, USA
[a)] Address all correspondence to this author. e-mail: sjh5899@psu.edu

Received: 21 March 2022; accepted: 4 May 2022

Two-dimensional (2D) layered materials as a new class of nanomaterial are characterized by a list of exotic properties. These layered materials are investigated widely in several biomedical applications. A comprehensive understanding of the state-of-the-art developments of 2D materials designed for multiple nanoplatforms will aid researchers in various fields to broaden the scope of biomedical applications. Here, we review the advances in 2D material-based biomedical applications. First, we introduce the classification and properties of 2D materials. Next, we summarize surface and structural engineering methods of 2D materials where we discuss surface functionalization, defect, and strain engineering, and creating heterostructures based on layered materials for biomedical applications. After that, we discuss different biomedical applications. Then, we briefly introduced the emerging role of machine learning (ML) as a technological advancement to boost biomedical platforms. Finally, the current challenges, opportunities, and prospects on 2D materials in biomedical applications are discussed.

Introduction

Over the past decade, nanoscience and nanotechnology have undergone significant advances in many interdisciplinary fields as more light is shed on its real-life applications with a special focus on biomedicine. Typically, nanomaterials are defined as a material of which dimension ranges from 1 to 100 nm creating an intermediate regime between atoms and bulk counterparts. 2D materials are especially desirable among various nanomaterials due to their layered structure with rich surface chemistry, establishing it as a hot research topic in the scientific community. 2D material can be generally described as a monolayer to a few-layered structure with a planar architecture [1–4]. Successful isolation of graphene back in 2004 followed by the synthesis of graphene-like 2D materials resulted in significant interest among researchers to explore the vibrant area of 2D materials which is applicable in biomedical applications [5–9].

The family of 2D materials includes graphene, hexagonal boron nitride (h-BN), transition metal dichalcogenides (TMDs), black phosphorous (BP), MXenes, etc. What makes 2D materials an exciting class of nanomaterial toward the biomedical field is their fascinating properties as compared to their bulk counterparts. 2D materials are especially attractive for biomedical applications as a consequence of their structure, large surface area, transport properties, ease of functionalization, biocompatibility, and adsorption capabilities, to name a few. Notably, 2D materials exhibit unique optical, mechanical, electrical, and magnetic properties that can be utilized in biomedical applications [10–15]. To unlock the true potential of 2D materials, scientists need to explore different avenues of synthesis, characterization, and applications of these materials. Although layered materials behold many merits, material properties can be modulated via the engineering of 2D materials to further enhance the sensing performances. In this regard, surface functionalization, defect and strain engineering, and creating 2D material-based heterostructures are explored as key-engineering pathways. As an artificial intelligent method, ML can provide insights into the synthesizability of 2D materials and the discovery of new materials by the means of structure–property relationships. In addition, ML has a critical role in analyzing raw sensing data by categorization, anomaly detection, noise reduction, target

identification, and pattern recognition to enable smart biotechnology [16]. As a result of these experimental and computational advances, 2D materials are explored in the landscape of biomedical applications such as bioimaging [17–19], drug delivery [18, 20–22], photothermal cancer therapy (PTT) [23–26], and tissue engineering (Fig. 1) [21, 27–29].

In this review, we attempt to shed further light on significant advances and state-of-the-art development of van der Waals (vdW) materials, especially with regard to their applicability to biomedical applications. We first start our discussion with the general classification of 2D materials encompassing distinctive features such as optical, electronic, and structural properties, and synthesis protocols. Then, we present engineering methods for 2D materials applicable in various fields. Next, we present a thorough discussion of several biomedical applications that can benefit from 2D materials. After that, we include a brief discussion on the emerging role of ML in the efficient design of 2D materials and how different computational models can be beneficial in biomedical applications. Finally, we discuss the challenges and future prospects of 2D materials for next-generation biosensors and other biomedical applications. We believe that this comprehensive review will stimulate and trigger the understanding of 2D materials as a potential candidate in emerging biomedical applications.

Classification and properties of 2D materials

The blooming of nanotechnology attracts enormous research interest toward developing novel nanomaterials with one or more dimensions in the scale of nanometers. Their physical properties are not only defined by the chemical compositions, but also by their dimensionality. Among low-dimensional materials, 2D materials, characterized as nanosheets connected by weak vdW forces between layers, are well suited for biomedical applications because of their superior surface-to-volume ratio, facilitating surface adsorption of analyte molecules during biosensing. The response to the adsorption event can be further enhanced by surface functionalization and defect engineering that contributes to improving the sensitivity. Furthermore, the 2D nature allows different layered materials to be assembled and integrated, creating multifunctional medical devices. Their tolerance to mechanical strain up to 10% without rapture makes them a candidate for flexible skin electronics [30]. As the synthesis techniques advanced, wafer-scale 2D materials can be easily produced with high quality and uniformity that are compatible with scalable productions.

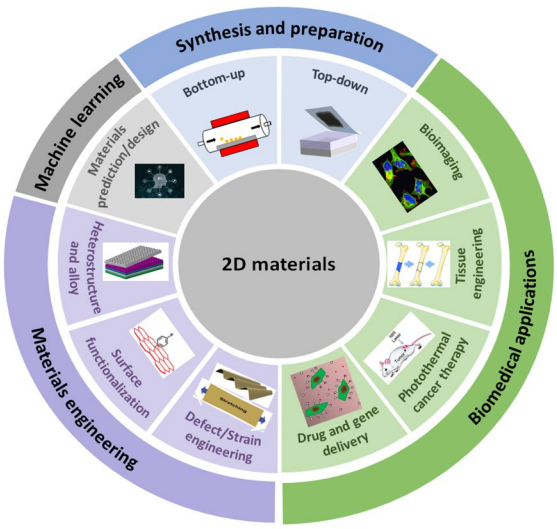

Figure 1: Schematic representation of synthesis and preparation, materials engineering, biomedical applications, and ML approaches applicable in 2D materials.

2D materials are widely explored for optical biosensing including graphene and other carbonic materials like graphene oxide (GO) and reduced graphene oxide (rGO), BP, TMDs, BN, MXenes, etc. They cover a wide range of the optical spectrum from visible-to-near-infrared (NIR) region with tunable band gaps and contrasting optical and electronic properties (Table 1). For instance, graphene is a conducting material composed of carbon atoms in a hexagonal lattice. It possesses superior thermal and electrical conductivity leading to strong charge transfer, which is beneficial for sensing based on graphene-enhanced Raman spectroscopy [31]. The oxidation of graphene by the Hummers method produces graphene oxide (GO), which is also often used for improving the biosensing performance through fluorescence quenching [32]. Compared to semi-metallic graphene, the band gap of GO can reach up to around 3.5 eV depending on the degree of oxidation [33]. Its band gap can be further modulated by reducing GO to form reduced graphene oxide (rGO) of which band gap varies from 1.00 to 1.96 eV [34]. The engineering of band structure and related optical properties can also be realized by changing the number of layers for a wide range of 2D materials, for example, BP and TMDs. Unlike graphene, BP exhibits strong anisotropy in optical properties because of its unique crystal structures. The band gap of BP changes significantly from 0.3 to 1.59 eV from bulk crystals to monolayers because of band structure modulation [2]. It hosts strong optical absorptions in the IR regime and high carrier mobility up to 1000 $cm^2\ V^{-1}\ s^{-1}$ [35]. In comparison, common TMDs monolayers have optical absorptions in the visible wavelength from 521 to 800 nm (2.38 to 1.55 eV) [36]. Besides, MXene is also an emerging type of 2D material that shows promise in optical biosensing [10]. It consists of layers of transition metal carbides, nitrides, or carbonitrides. The abundance of surface functionalization groups, such as –O, –OH, and –F, upon etching makes the surface adsorption of biological molecules easier to happen for MXenes [4]. Table 1

TABLE 1: Crystal structures, bulk band gap, dielectric constant, and carrier mobility of different 2D materials.

2D material	Graphene	GO	BP	TMDs	h-BN	MXenes
Crystal structure(top and side views)	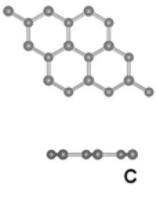	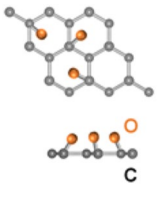	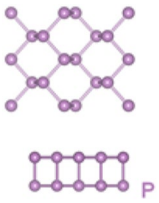	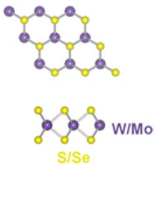	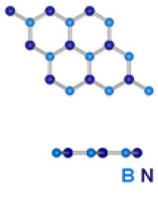	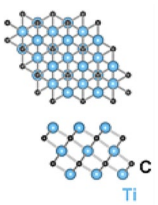
Bulk bandgap (1L bandgap)	0 eV	2.2 eV [34]	0.3 eV [2] (2 eV) [37]	1.1–1.4 eV [38] (1.6–2.4 eV) [39]	5.9 eV [40]	0–1.8 eV [41]
Dielectric constant at optical frequency	6.9 [42]	30–50 [43]	2.9 [44]	6.3–7.5 [45]	3.3 [45]	1–4 [46]
Carrier mobility	10^5 cm^2/V s [47]	N/A	10^3 cm^2/V s [37]	10–90 cm^2/V s [48]	N/A	1–10^5 cm^2/V s [49]

compares Crystal structures, bulk band gap, dielectric constant, and carrier mobility of different 2D materials.

The practical application of 2D materials in biomedical applications is also enabled by the advances in producing large-area high-quality 2D materials. Chemical vapor deposition (CVD) and metal–organic CVD (MOCVD) are prevalent methods to synthesize wafer-scale 2D materials beyond graphene [50, 51]. Efforts have been made toward ensuring the uniform orientation and increasing the size of the domains, of which mechanism is guided by thermodynamics and kinetics [52]. In contrast, molecular beam epitaxy utilizes high-purity elemental sources and ultrahigh vacuum. The in situ characterizations in MBE offer better control of the number of layers compared with CVD [53]. It is also worth noting that 2D monolayers with a size up to millimeters have been realized by mechanical exfoliation using adhesive layers that show better chemical affinity with the 2D materials [54–56].

Surface and structural engineering of 2D materials

The rapidly expanding family of vdW materials with unique optoelectronic properties has remodeled the future of health-relevant sensing modalities. Achieving precise control over the surface chemistry of 2D materials is key for guaranteeing high standards in biomedical applications. Recent works have demonstrated unique engineering approaches including surface functionalization, doping, defect and strain engineering, multilayer stacking, and incorporating with plasmonic nanoparticles, quantum dots (QDs), and functional polymers to broaden the scope of biomedical applications by creating devices with enhanced performance. Here, we briefly highlight the above 2D material engineering pathways for utility in biomedical applications.

Surface functionalization

Surface functionalization can be used to endow properties such as stability and biocompatibility for multifunction capacity. Pristine 2D materials are rarely used in biomedical applications due to the lack of targeting ability. Functionalization strategies have been well accepted to introduce colloidal stability and biocompatibility in order to fuel biomedical applications. Graphene as a widely explored material can be functionalized at the basal plane and edges. Typically, for graphene, π–π interactions can facilitate the interface between the basal plane and foreign molecules, while edges with dangling bonds can form strong interactions with biomolecules [57]. GO is characterized by abundant reactive groups such as carboxylic acid groups, hydroxides, and epoxides which are biocompatible, allowing efficient coupling with biomolecules, biological cells, and tissues. In this context, various biosensors can be developed based on the fact that surface functionalization could lead to changes in the charge density, electronic mobility, and mechanical strain [58]. Toward this goal, modification of GO by polyethylene glycol (PEG) has been widely utilized in targeted applications (Fig. 2a) [18, 21, 59]. Similar strategies can be extended for the surface modification of rGO as well as nanoparticles (NPs) decorated GO and rGO. Other functional groups, including poly-L-lysine (PLL) [60] and chitosan [20], have been explored as suitable candidates for the surface functionalization of GO [Fig. 2(b)].

Atomically thin BP has attracted significant attention due to its unique physical properties, leading to a plethora of applications such as drug delivery, gene delivery, PTT, bioimaging, and tissue engineering [61–64]. A fundamental obstacle hindering the applications of BP is its poor air stability, mainly arising due to the non-bonding lone pair electrons of P atoms on their surface, resulting in compositional and physical changes. Therefore, it is critical to attach foreign moieties to occupy the lone pair to assure better stability in a physiological

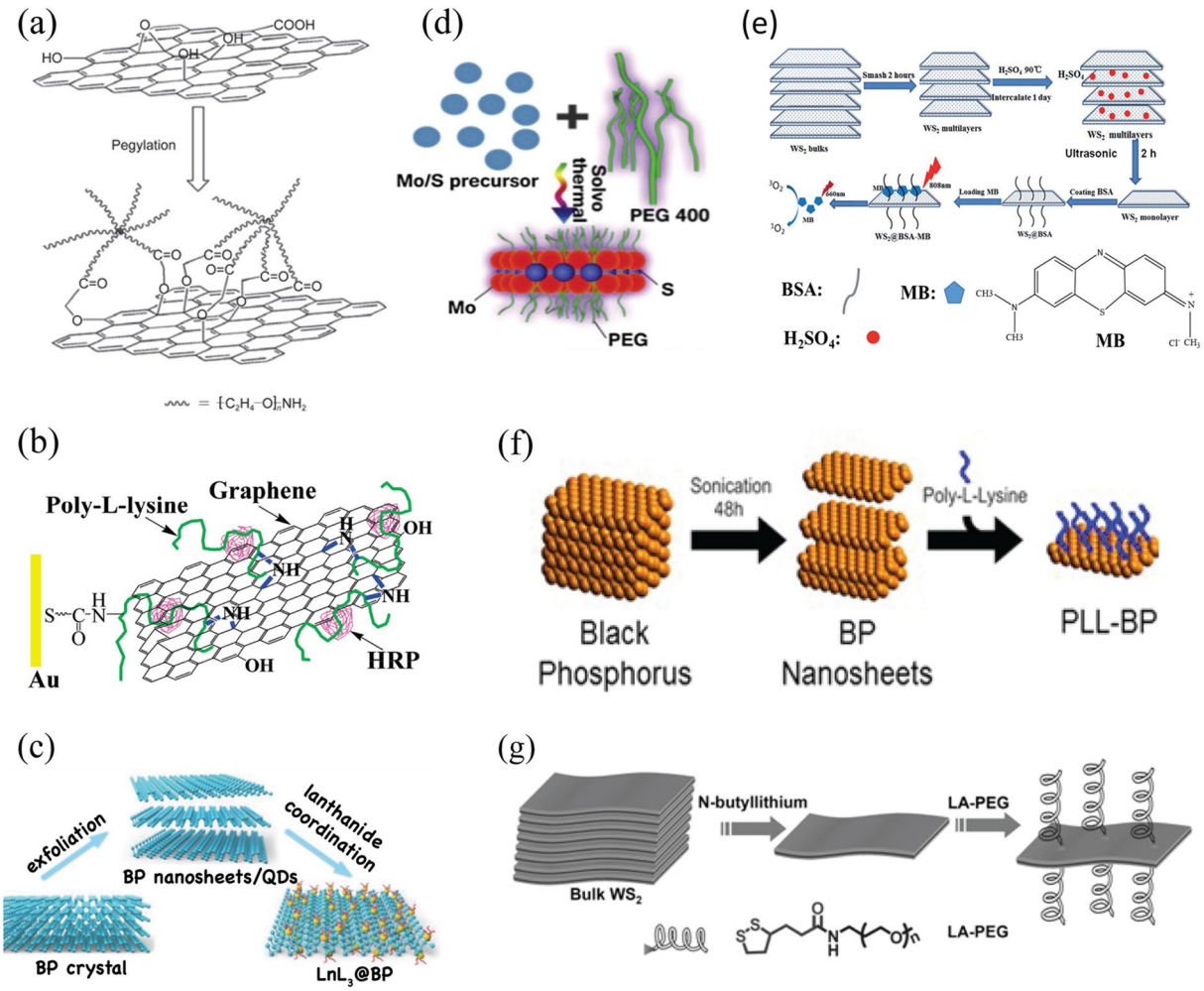

Figure 2: Schematic representation of surface functionalization in 2D materials. (a) PEGylation of GO by PEG stars. Adapted with permission from Reference [18] © 2008 Springer. (b) Graphene-PLL Synthesis. Adapted with permission from Reference [60] © 2009 American Chemical Society. (c) Synthesis of lanthanide-coordinated BP nanosheets. Adapted with permission from Reference [65] © 2018 Wiley Online Library. (d) Solvothermal synthesis procedure of MoS_2-PEG nanosheets. Adapted with permission from Reference [69] © 2015 Elsevier. (e) Synthesis procedure of WS_2 nanosheets and their application as a multifunctional photosensitizer delivery system. Adapted with permission from Reference [72] © 2014 Royal Society of Chemistry. (f) Liquid-phase exfoliation of BP nanosheets and their surface modification with PLL. Adapted with permission from Reference [68] © 2016 American Chemical Society. (g) Exfoliation and PEGylation of WS_2 nanosheets. Adapted with permission from Reference [17] © 2013 Wiley Online Library.

environment. Multiple efforts have been devoted to improving the stability of BP, and some of the recent examples aiming at this goal include lanthanide sulfonate complexes [65], titanium sulfonate ligands [66], and alkyl halides [67]. In these examples, different coordinations such as P-Ln, P-Ti, and P-C occupy the lone pair of the electrons of phosphorous, preventing exposure to air and water [Fig. 2(c)]. Moreover, functionalized BP showed excellent stability in air and during dispersion in water as compared to bare BP due to suppressed reactivity. In addition, Kumar et al. reported noncovalent modification of BP with PLL via Coulombic interactions for label-free electrochemical-sensing platform for myoglobin (Mb) [Fig. 2(f)] [68]. Here, functionalized layered material plays a vital role in facilitating binding with anti-Mb DNA aptamers, eventually resulting in a superior detection limit of 0.524 pg/mL toward Mb.

TMDs are another kind of layered materials that can broaden its scope by chemical functionalization. To date, various types of functional materials, including biocompatible polymers [17, 69–71], biological molecules [25, 72, 73], and inorganic nanomaterials [11, 74] have been utilized for surface modification of TMDs to meet the demands of biological applications [Fig. 2(d), (e), (g)]. In particular, TMDs prepared by mechanical exfoliation are characterized by a large number of defects due to the loss of atoms during the hard exfoliation process, providing an opportunity for surface functionalization via covalent

attachment [57]. These findings have revealed that due to the linker attachment, overall performances such as the efficacy of PTT, high drug-loading capacity, and high drug-releasing capacity are significantly improved while exhibiting much higher biocompatibility. Additionally, the surface of MXenes can be modified with NPs [75–77], PEG [75], and soybean phospholipid (SP) [78] to realize outstanding performances in biological media. All these findings demonstrate that the functionalization of 2D materials paves a path for unique opportunities and remarkable properties that bare 2D materials could not provide to expand the opportunities in the biomedical field.

Defect and strain engineering

The existence of defect states in 2D materials has proved to enhance the catalytic activity, improve the optical properties of layered materials [79], and improve the sensitivity and selectivity of biosensors. Both defect and strain engineering can contribute to such defect states in 2D materials. Defect engineering can be achieved by introducing intrinsic defects (vacancy, active edge sites, etc.) and dopants (metal dopant, heteroatom dopant, etc.). Introducing crystalline imperfections into 2D materials is commonly achieved by electron or ion irradiation [80–83], plasma treatment [84], and thermal treatment [Fig. 3(a)–(d)] [85–87]. Focused ion beam (FIB) is a decent way to realize controllable density and distribution of defects. Both chalcogen and metal vacancies and even nanopores can be created in thin TMDs flakes by FIB [88]. Plasma treatment is a more macroscopic means of defect creation by surface modification, introducing doping as well as layer thinning [89]. Atomic-scale defects in WS_2 and MoS_2 arise after exposure to Argon plasma, resulting in a new defect-related photoluminescence (PL) peak at ~ 0.1 eV lower than the intrinsic A-exciton emission [90]. Thermal treatment under a particular atmosphere can also introduce a controllable number of defects and has the advantage of high throughput [85, 86, 91].

Strain engineering offers another degree of freedom to tune the lattice and electronic structures of 2D materials. Sources of strain can be summarized into engineered substrates and local heterogeneity. Atomically thin 2D materials are easy to deform in the out-of-plane direction when external forces are applied, giving rise to the presence of strain [92]. By integrating 2D materials with engineered substrates like flexible or patterned substrates, strain can be introduced in a controllable manner. When using flexible substrates, strain mainly comes from the mismatch of elastic modulus between 2D materials and the chosen flexible substrates [93, 94]. There are many types of available flexible substrates such as polydimethylsiloxane (PDMS), polycarbonate

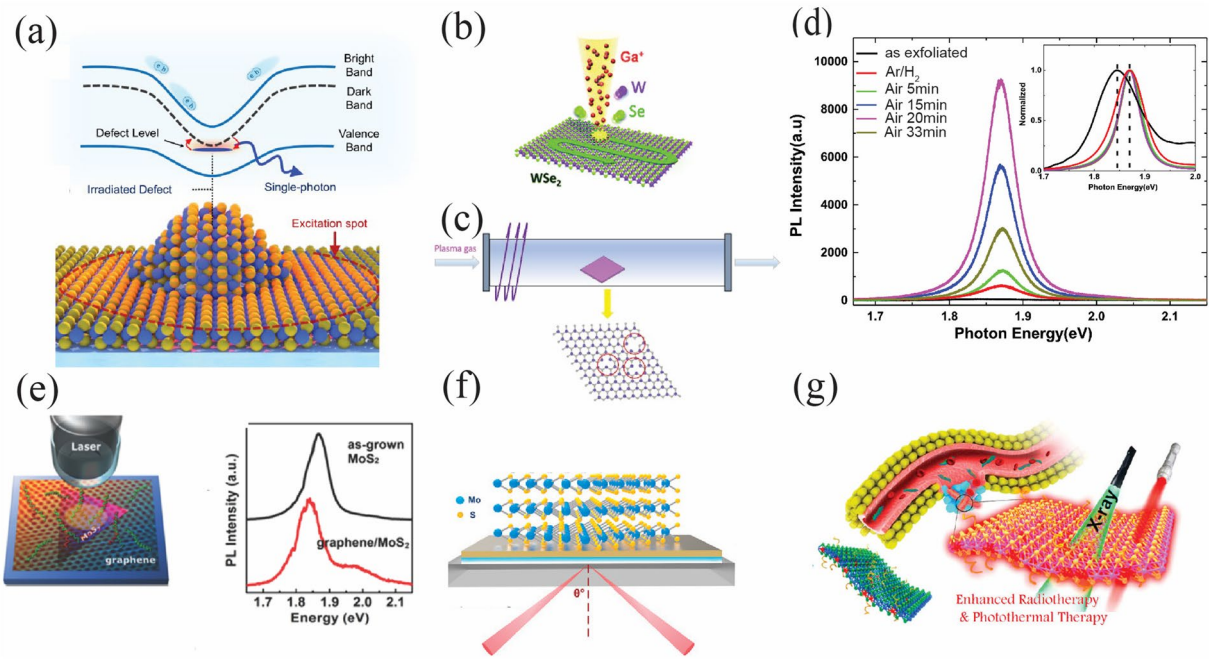

Figure 3: Illustration of structural-engineering approaches. (a) Schematic illustration of defect state in WSe_2 monolayer. Adapted with permission from Reference [83] © 2022 Springer Nature Limited. (b) Defect creation from Focus Ion Beam. Adapted with permission from Reference [81] © 2020 Royal Society of Chemistry. (c) Defect creation from plasma treatment. (d) Defect-assisted PL enhancement in monolayer MoS_2 after thermal treatment. Adapted with permission from Reference [87] © 2014 AIP Publishing. (e) Detection of DNA using MoS_2/graphene heterostructure, adapted with permission from Reference [101] © 2014 Wiley Online Library. (f) Schematic of MoS_2/graphene-enhanced SPR biosensor. Adapted with permission from Reference [102] © 2014 Elsevier. (g) Enhanced Radiotherapy and PTT by using Metal-ion-doped WS_2. Adapted with permission from Reference [105] © 2015 American Chemical Society.

(PC), and polyethylene terephthalate (PET). When 2D materials are transferred onto the patterned substrates, the surface features of substrates like nanopillars, trenches, and ripples will result in different strain states [95]. Apart from external forces, local heterogeneity of the 2D materials can also induce strain. Bubbles [96] and wrinkles [97] are very commonly seen in a 2D material sample due to the aggregation of air and other impurities like hydrocarbon adsorbed between the 2D material and substrate. Both patterned substrates and local heterogeneities give rise to strain 'hot spots,' resulting in the tuning of local optical properties such as single-photon emitters [83, 98], and enhanced nonlinear responses [99, 100].

Design of heterostructures

The large surface-area-to-volume ratio of 2D materials makes them perfect candidates for biomedical applications. Furthermore, by integrating with other nanomaterials, it is possible to tailor the materials' electrical, optical, and other properties, giving rise to more possibilities of biomedical application. 2D heterostructures, which are assembled layer-by-layer from certain 2D materials, provide more possibilities of achieving better performing biosensors. Loan et al. fabricated a MoS_2-graphene heterostructure with an ultrahigh sensibility of DNA molecules [Fig. 3(e)] [101]. Zeng et al. proposed a surface plasmonic resonance (SPR) system consisting of graphene-MoS_2 heterostructure and an additional layer of gold (Au) [Fig. 3(f)] [102].

2D materials nanocomposites are also proved to have enhanced analytical performance in biomedical applications [103]. Metal-structure-decorated 2D material composites improve the biosensing capabilities of electrochemical biosensors, benefited from the biocompatibility of the metal structures such as AuNPs and their ability to immobilize biological recognition elements as well as facilitated electron and mass transfer [104]. Metal-ion-doped 2D nanoflakes show the potential of realizing PTT and enhancing radiation therapy for tumor treatment [Fig. 3(g)] [105]. Li et al. reported tin disulfide (SnS_2) decorated with Au or bimetallic Pt–Au NPs results in larger current responses compared to the pristine ones in the amperometric glucose biosensor [106]. Currently, the biomedical applications of 2D vdWs still have many obstacles, for example, device mass production, durability, cost, etc. And there is still a lack of thorough understanding of the interaction mechanism of chemicals and biomolecules at 2D interfaces.

Biomedical applications of 2D materials

Various 2D materials have been investigated and examined for a wide variety of biomedical applications due to their excellent chemical and physical properties. The rationale behind using these materials in the biomedical field lies in the unique features that these materials offer, such as atomic-thin structure, broad surface area, the abundance of chemically active sites, large number of surface contacts, and quantum confinement effect, to name a few. Additionally, chemical and optical properties play a critical role in respective applications. On the other hand, interactive characteristics between 2D materials and biomolecules such as hydrogen bonding, electrostatic interactions, and hydrophobic interactions serve as driving forces to determine biological functions. In this section, we focused on representative biomedical applications of 2D materials.

Bioimaging

Bioimaging is an important field in research and clinical applications allowing visualization and monitoring of biological processes with the help of optical properties of materials. This is especially important in theranostics to ensure proper identification of tissues before treatments are started. In most cases, organic dye molecules were used as probes due to their high quantum efficiency, but they suffer from photobleaching, calling for alternative approaches. In this avenue, nanomaterials have proven their efficacy in bioimaging, and 2D materials are also researched heavily as a potential metal-free candidate in various bioimaging modalities. Apart from multicolor fluorescent imaging, other imaging platforms such as photoacoustic imaging (PA), magnetic resonance imaging (MRI), computed tomography imaging (CT), surface-enhanced Raman scattering (SERS) imaging, positron emission-computed tomography imaging (PET), and multimodal imaging techniques are significantly improved for the understanding of various cellular activities and functions as well as monitoring of internal body structures. In this section, 2D material-based bioimaging applications are briefly discussed.

CT imaging is one of the most routinely applied techniques, which relies on the difference in contrast between lesions and tissues to reconstruct the cross-sectional images. Among the 2D-layered material family, TMDs and MXenes are ideal candidates for CT imaging as compared to carbon-based materials due to the high atomic-number elements that can provide excellent X-ray attenuation ability. Therefore, it is essential to use functionalized graphene to realize graphene-based 2D materials in CT imaging. For example, the application of GO as a contrast agent in CT was demonstrated with the Au microcapsule deposition technique [107]. Here, AuNPs were served as a contrast agent to enhance CT imaging while GO serves as a better absorber in the NIR range for PTT. Particularly, PEGylated WS_2 nanosheets were demonstrated as a bimodal contrast agent for enhanced X-ray CT and PA tomography (PAT) bimodal imaging

of tumors [17]. As PAT imaging is based on acoustic detection of optical absorption, PEG-WS_2 nanosheets with high NIR absorbance appear to be an ideal contrast agent providing uniform signal distribution inside the tumor structure. Additionally, elaboratively designed nanocomposites such as BSA-coated WS_2 [72] and PEGylated MoS_2/Bi_2S_3 [108] also demonstrated strong X-ray attenuation, providing sensitive CT-imaging capability. Other 2D family members such as MXenes and BP were also investigated as desirable candidates for PA contrast agents. For example, SP-modified Ti_3C_2 nanosheets (Ti_3C_2-SP) were prepared by Han and coworkers, demonstrating multiple functionalities [78]. They found that Ti_3C_2-SP has high PA signal under 808 nm light irradiation and displayed a substantial increase in signal with increasing concentration of Ti_3C_2-SP. Furthermore, the PA-imaging capability of nanocomposite was illustrated with 4T1 tumor-bearing mice. The collected data suggested enhancing the PA contrast in the tumor within 4 h followed by the decay of the signal indicating gradual accumulation and excretion of Ti_3C_2-SP, further implying high biosafety for clinical applications. Recent work has been performed to advance the use of PA imaging in the NIR-II (1000–1700 nm) window in addition to the NIR-I (700–950 nm) window [109]. Apart from MXenes, Yang et al. developed modified BP nanosheets via π–π stacking strategy, opening window for a series of applications [63]. In particular, modified nanosheets showed excellent in vivo PA-imaging signals in the tumor.

PET is another imaging technique based on detecting gamma rays as a result of introducing radiotracers into the body. Some engineering-designed 2D materials, such as graphene-based derivatives and TMDs were reported as key contrast agents [110, 111]. In a demonstration by Dong et al., a multifunctional MoS_2-based nanoplatform was synthesized by decorating with hyaluronic acid (HLA) and polyethyleneimine (PEI), which is applicable in PET imaging of MCF-7-ADR tumor in mice [110]. They successfully labeled the nanocomposite with ^{64}Cu to realize PET imaging of the tumor-bearing mice. In another work, Liu and coworkers uncovered the potential of radiolabeled MoS_2-iron oxide (MoS_2-IO) to enable PET imaging [112]. Utilizing radiolabeling, these researchers successfully demonstrated tumor accumulation of the nanocomposite. In another work, the same research group reported iron selenide ($FeSe_2$) decorated bismuth selenide (Bi_2Se_3) nanosheets, revealing the applicability of TMDs as sophisticated bioimaging modalities for disease diagnosis [113]. Apart from TMDs, graphene-based derivatives were found immensely useful in PET imaging. Recently, Cai and coworkers reported ^{64}Cu radiolabeling of GO taking advantage of interactions between Cu and the π electrons of GO [111]. Traditional radiolabeling strategies involved chelator conjugation (DOTA (1,4,7,10-tetraazacyclododecane-1,4,7,10-tetraacetic acid) or NOTA (1,4,7-triazacyclononane-1,4,7-triacetic acid)) as an essential step. But with this novel approach, researchers were able to preserve the pharmacokinetics of GO. In addition, they explored the labeling yield of PEGylated rGO and found out that it is superior to GO mainly due to the high concentration of π electrons in rGO. They demonstrated that this novel platform could provide informative results in PET imaging

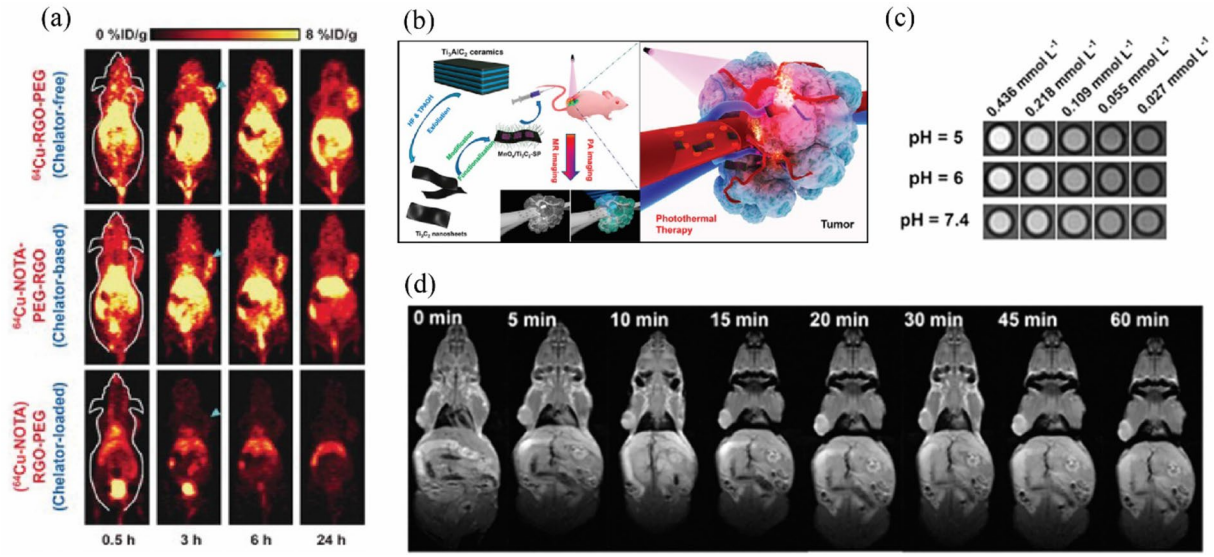

Figure 4: Different bioimaging modalities applicable in 2D materials. (a) Serial coronal PET images at different time points post-injection of ^{64}Cu-RGO-PEG, ^{64}Cu-NOTA-PEG-RGO, and (^{64}Cu-NOTA)-rGO-PEG acquired in 4T1 tumor-bearing mice. Adapted with permission from Reference [111] © 2017 Wiley Online Library. (b), (c), and (d) Schematic illustration of theranostic functions of MnO_x/Ti_3C_2–SP composite nanosheets, in vitro T_1-weighted MR imaging of MnO_x/Ti_3C_2–SP nanosheets in buffer solution at different pH values, and T_1-weighted imaging at different time intervals. Adapted with permission from Reference [115] © 2017 American Chemical Society.

when tested on 4T1 breast tumor-bearing mice as shown in Fig. 4(a). Moreover, Kai and coworkers used ^{66}Ga-labeled PEG-linked nGO for tumor-targeted PET imaging [114]. Overall, the presence of heavy elements and higher PT conversion efficiency established versatile 2D-layered materials as rising stars in CT and PAT imaging, respectively.

MRI is a powerful technique capable of providing morphological and functional information. As there is growing attention to exploring novel MRI contrast agents, 2D materials are also investigated as potential agents by integrating magnetic species. Recently, Dai and coworkers showed the potential of MXenes as MRI contrast agent by in situ growth of manganese oxide (MnO_x) NPs on the surface of nanosheets (Ta_4C_3 and Ti_3C_2) as depicted in Fig. 4(b) [77, 115]. They found that decoration of MnO_x over MXene nanosheets leads to pH-responsive and glutathione-sensitive T_1-weighted MRI. Especially, the pH responsiveness plays a significant role in enhanced T_1-weighted MRI performance as cleavage of Mn–O bonds under mild acidic conditions leads to the release of Mn ions [Fig. 4(c)]. They were able to observe contrast-enhanced MRI signal (remarkable brightness effect) attributed to the efficient accumulation of the nanocomposite by enhanced permeability and retention (EPR) effect and acidic environment of tumors [Fig. 4(d)]. Inspired by that the Chen group extended the concept of in situ growth of nanocrystals to design superparamagnetic 2D Ti_3C_2 MXenes for theranostic applications [13]. They developed the nanocomposite by in situ growth of iron (II, III) oxide (Fe_3O_4) nanoparticles (IONPs) on the surface of Ti_3C_2 followed by functionalization with SP (Ti_3C_2-IONPs-SP). IONPs act as an efficient contrast agent for MRI illustrated by high T_2 relaxivity up to 394.2 mM^{-2} s^{-1}. Recent work has been done to advance the use of other 2D materials as therapeutic agents by integrating diverse functionalities. Yang et al. developed a novel MRI nanoplatform using assembly of iron (III) oxide (Fe_2O_3) and AuNPs on BP (BPs@Au@Fe_2O_3) [116]. The potential of nanocomposite as a T_2-weighted MRI contrast agent was examined with tumor-bearing mice. In addition, multimodal imaging techniques are rapidly gaining significant interest when the system under investigation becomes more complex. To date, several reports aiming at multimodal imaging applications of 2D-layered materials are available in the literature to expand the capabilities of single-imaging modalities by combining several advantages into one platform. In-depth discussion of 2D material-based multimodal imaging techniques is out of the scope of this review, and readers are encouraged to read other articles on this topic [117, 118].

Besides CT, PA, PET, and MRI, other bioimaging techniques assisted by 2D materials have been widely studied, such as SERS imaging, coherent anti-stokes Raman scattering (CARS) imaging, stimulated Raman spectroscopy (SRS) imaging, nonlinear optical imaging, and SPR [31, 119–127].

Drug delivery

Many nanoplatforms have been employed for targeted drug delivery using NPs loaded with drugs to increase the local concentration of the drug at the target site and minimize any side effects. 2D materials, due to their atomic thickness and high specific surface area, are excellent candidates for targeted drug delivery. The ample surface enables drugs and other molecules to efficiently anchor on the surface and get delivered to the target site [128, 129]. Graphene and its derivatives, including GO and rGO, were among the first 2D materials to be explored as drug delivery carriers due to their surface properties, including delocalized π electrons on the surface enabling cancer drugs to anchor using π–π interactions [18, 22]. It also allowed the surface functionalization of the graphene surface, especially in GO and rGO, enabling drug loading by means of covalent bonding. GO has much broader applications in drug delivery due to the presence of the hydroxy and epoxide functional groups enabling efficient physisorption or chemisorption of drugs with high biocompatibility and stability [130]. These materials are often loaded with drugs like doxorubicin (DOX), a chemotherapy drug which slows down the growth of cancer cells, to evaluate their drug delivery attributes.

Recently, Huang et al. prepared silicon contact lenses loaded with GO and HLA, a drop solution used to treat dry eye syndrome, with sustained release of HLA up to 96 h. The lenses were safe in an ocular irritation study with increased water retention preventing dry eyes [131]. A GO-sodium alginate (SA) composite was formed using Ca^{2+} as the crosslinker to prepare a freeze-dried SA-CA^{2+}-GO hybrid which functioned as a drug carrier for methotrexate (MTX), as shown in Fig. 5(a). This hybrid carrier showed superb electro and pH-responsive release of MTX due to the excellent conductivity of GO and pH response of SA, respectively [132]. Further functionalization of GO and rGO is a great method to improve its biocompatibility and the choice of drugs to be delivered [133]. A multifunctional rGO hybrid can be created by reacting rGO with dopamine (DA), auric chloride, sodium borohydride ($NaBH_4$), and DOX successively to create an rGO/DA/AuNP/DOX hybrid nanomaterial [134]. The nanomaterial displayed a pH-dependent DOX release with an initial loading capacity of 0.852 mg/mg of rGO/DA/AuNP/DOX material and PT properties, as shown in Fig. 5(b). Functionalized GO has also been used as a therapeutic nanomaterial against Parkinson's disease (PD) by loading with Puerarin (Pue). This natural anti-PD compound otherwise cannot be used by itself due to its inadequate bioavailability and limited transfer through the blood–brain barrier (BBB) [135]. They created a Pue-loaded GO nanosheets with excellent drug-loading ability and biocompatibility, which crossed the BBB using lactoferrin as the targeting ligand [Fig. 5(c)]. In vitro and in vivo studies in mice proved this hybrid drug delivery system as an effective

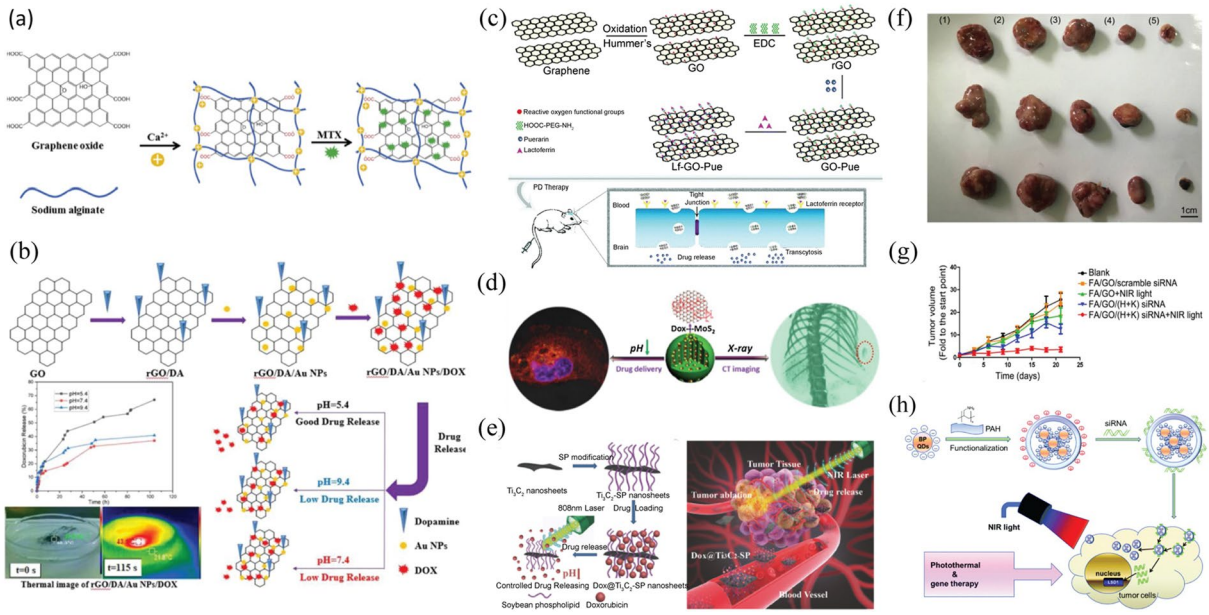

Figure 5: Different drug and gene delivery pathways based on 2D materials. (a) Schematic illustrating the making of MTX-loaded SA-CA^{2+}-GO hybrids. Adapted with permission from Reference [132] © 2020 Elsevier. (b) Preparation of rGO/DA/AuNP/DOX hybrid nanomaterial with pH-dependent DOX drug release Adapted with permission from Reference [134] © 2022 Elsevier. (c) Synthesis of Lf-GO-Pue hybrid for targeted treatment of PD. Adapted with permission from Reference [135] © 2021 Royal Society of Chemistry. (d) Schematic illustration of MoS_2 NDs-incorporated MSN for pH-sensitive drug delivery and CT imaging. Adapted with permission from Reference [137] © 2021 Elsevier. (e) Surface modification of Ti_3C_2 nanosheets by SP, their further DOX drug loading, and responsive drug releasing by external irradiation or internal pH change. Adapted with permission from Reference [78] © 2018 Wiley. (f) Anti-tumor activity of multifunctionalized PEG-GO nanomaterial with representative tumor tissue images of mice treated with (1) PBS, (2) FA/GO/scramble siRNA, (3) FA/GO with NIR light, (4) FA/GO/(H + K) siRNA, or (5) FA/GO/(H + K) siRNA with NIR light. Adapted with permission from Reference [147] © 2017 Ivyspring International. (g) Relative changes in tumor volume over time after mice treated with multifunctionalized PEG-GO nanomaterial. Adapted with permission from Reference [147] © 2017 Ivyspring International. (h) Schematic illustration for combined PT and gene delivery for human ovarian cancer cells using BPQD-PAH loaded with siRNA. Adapted with permission from Reference [148] © 2017 Royal Society of Chemistry.

therapy for PD. These examples highlight the use of GO and rGO as excellent nanocarriers for drug delivery applications.

MoS_2 as a widely investigated TMD shows interesting drug delivery applications and a high PT response. Moreover, the presence of unsaturated d-orbitals, active edges, and sulfur vacancies enable the functionalization of MoS2 nanosheets, reducing their cytotoxicity [136]. Recently, Chen et al. realized this by incorporating monodispersed MoS_2 nanodots (NDs) on mesoporous silica nanospheres (MSN) using a solvothermal reaction [137]. The MoS_2 ND functioned as anchoring sites for the DOX drug and had a pH-responsive drug release based on electrostatic interaction with the DOX molecules. The dispersed NDs also acted as biocompatible contrast agents in CT scan imaging of breast cancer and glioma tumors in mice, as shown in Fig. 5(d).

MXenes are also an excellent candidate material for targeted drug delivery due to their surface functional groups enabling modification, inertness, and very high capacity for drug loading [138]. Ti_3C_2 can be easily functionalized by the hydroxyl group, which increases its solubility and the cationic drug-loading capacity [19]. Recently, Han et al. developed Ti_3C_2 functionalized by SP, which enables easy transport of MXene in blood vessels and increased its surface area [78]. This hybrid was then loaded with DOX drug showing up to 211% loading capacity with pH-responsive or NIR laser-triggered drug release, as shown in Fig. 5(e). Both PT ablation and chemotherapy approaches were demonstrated in vivo and in vitro leading to efficient tumor eradication. The MXene hybrid also showed high histocompatibility and was easily excreted out of the system, thus, highlighting its potential use in drug delivery applications.

Gene and protein delivery

Gene delivery is an alternate approach to traditional treatments for genetic diseases and involves replacing the improperly functioning and disease-causing genes with new nucleic acid polymers, which function correctly and, thus, prevent the development of genetic diseases [139, 140]. Tremendous research efforts have been applied to develop gene delivery therapy for viral, cardiovascular, cancer, Parkinson's, and other genetic diseases [141, 142]. This approach requires genetic material and a gene delivery agent which can protect the genes from lysosome degradation and deliver them to the target site while being non-toxic and non-immunogenic.

Thus, the genetic material, i.e., DNA and RNA, needs to be encapsulated by the gene delivery agent through electrostatic interactions [143]. This therapeutic approach involves the use of siRNA (small interfering RNA), which regulates the expression of pathogenic proteins by destroying the target messenger RNA (mRNA), and this approach is termed RNA interference (RNAi) [144]. NPs and 2D materials can act as effective carrier agents for siRNA due to their large surface area, ability to functionalize their surface, and biocompatibility.

Free nucleic acids are very fragile; they decompose quickly and have limited absorption due to their negative charge. GO also has a negative charge due to the presence of carboxyl groups on its surface. Thus, to effectively utilize GO as a gene carrier agent, it needs to be functionalized by positively charged polymers like PEI and PEG [145]. PEI-rGO hybrids have been shown to form complexes with siRNA using the gel electrophoresis method and have since become an excellent platform material for gene silencing [146]. Yin et al. prepared PEGylated GO nanosheets for PT and gene delivery for pancreatic cancer [147]. The authors used the multifunctionalized GO nanosheets to deliver HDAC1 and k-Ras siRNAs to target a specific pancreatic cancer cell MIA PaCa-2 in mice. They could silence both the HDAC1 and k-Ras genes, leading to cell growth inhibition in treated cancer cells. Further, combining NIR light PT with gene delivery led to an 80% reduction in tumor growth compared to untreated samples, as shown in Fig. 5(f) and (g). GO could also be easily metabolized in the mouse without any side effects.

BP is another 2D material that has been utilized for gene delivery applications due to its high loading capacity, biocompatibility, and biodegradability. Yin et al. first used BPQDs-based nanocarriers functionalized with polyelectrolyte polymers (eg-poly(allylamine hydrochloride) (PAH)) to deliver siRNA into human ovarian cancer cells (eg-PA-1) [148]. The BP-PAH complex showed superior transfection efficiency with significant LSD1 (lysine-specific demethylase 1) mRNA suppression in PA-1 cells. BPQD possessed low cytotoxicity even at higher concentrations and inhibited the tumor growth by 80% in combination with NIR phototherapy. The scheme for the experiment is shown in Fig. 5(h). BP nanosheets have also been used for the delivery and release of CRISPR/Cas9 ribonucleoprotein to the cytoplasm for in vivo and in vitro genome editing and genome silencing [61].

Protein therapy utilizes the delivery of precisely structured proteins to target sites with well-known biological effects and is an alternative form of treatment to gene delivery. Similar to gene therapy, the proteins used here are unstable with a short lifespan and need a suitable carrier to succeed as a therapeutic. Rebekah et al. developed a magnetic nanoparticle composite as a carrier for bovine serum albumin (BSA) protein [12]. Sodium dodecyl sulfate–polyacrylamide gel electrophoresis (SDS-PAGE) analysis of Fe-GO-BSA and Fe-GO-CS-BSA solution showed no change after exposing them to trypsin for 3 h, thus, indicating that the protein remained intact, and the carrier protected it from enzymatic cleavage. More research is needed in engineering less cytotoxic and high drug-loading 2D materials hybrid for their use as nonviral vectors for gene and protein delivery.

Photothermal cancer therapy

Cancer is one of the deadliest diseases worldwide. Therefore, early diagnosis and treatment of this devastating disease are of paramount importance in medicine. Conventional treatments include chemotherapy, radiotherapy, hormonal therapy, immunotherapy, and surgery, but their long-term success rate is prohibited by efficacy and side effects on normal tissues. Due to these drawbacks researchers and medical professionals have made tremendous innovations based on alternative approaches such as nanomaterial-based therapies. PTT has advanced rapidly as a novel technique with a unique mechanism of cancer therapy. Briefly, this involves the conversion of light to thermal energy after exposure to a suitable PT agent to NIR radiation. This triggers the death of cancer cells while showing minimal invasiveness to normal tissues or cells. Many nanomaterials have effective light to heat conversion efficiency, and emerging 2D materials are also investigated as influential candidates. Such an interest in 2D materials is mainly due to their multifunctional potential ranging from tunable optical properties to ease of surface modification and plasmonic properties in the NIR region. Moreover, significant research interest is also devoted to designing 2D materials toward utilization in the NIR-II region compared to the widely studied NIR-I biological window. This is mainly due to higher power safety limits and desirable penetration depth into tumors buried deep in biological tissues [76]. Additionally, multiple imaging techniques can be employed to achieve better therapeutic efficacy of PTT. Another research area is integrating multifunctional nanomaterials with 2D materials for combined therapies such as PTT-Photodynamic therapy (PDT), PTT-Chemotherapy, and PTT-Immunotherapy to eliminate cancer cells. Herein, we summarize recent research progress of layered materials in the field of PTT.

Graphene and its family members, such as GO and rGO, have been actively examined in PTT-related applications due to strong optical absorption in the NIR region. In order to enhance the biocompatibility and dispersity of 2D materials, the grafting of layered materials with PEG is widely used. Gu and coworkers developed a GO-based nanocarrier by attaching bifunctional PEG followed by a furin-cleavable peptide for combined cancer treatment [149]. Here, PEG serves as a bridge between carboxylate GO and furin-cleavable peptides while improving the dispersity and stability of GO.

Alternatively, attachment of other biomolecules and polymers is also utilized in the surface functionalization of graphene-related materials. For example, porphyrin functionalized GO (PGO) demonstrated higher stability in an aqueous medium as compared to GO and efficient PT conversion efficiency of ablating brain cancer cells [150]. Liu and coworkers demonstrated in vivo PTT of cancer by using nanographene sheets [59]. They observed a significant increase in PEGylated nanographene sheets temperature upon irradiation of 808 nm light at a power density of 2 W cm^{-2} with the relatively unchanged temperature of the water sample as a control. They were able to photoablate U87MG cancer cells in a mouse by this approach. To improve the GO-based PTT, GO can be reduced to form rGO. In this regard, Dai and coworkers developed a PEGylated reduced nano-GO (nRGO) based PT agent exhibiting sixfold higher NIR absorption than nonreduced nano-GO (nGO) for eradicating cancer [26]. Here, higher NIR absorption was attributed to partial restoration of aromaticity. Furthermore, they observed a concentration-dependent increase in temperature for nRGO and nGO where the former showed an increase in temperature more than 50 °C and later showed maximum temperature up to 36 °C. In another demonstration, Kim and coworkers prepared functionalized rGO-based nanotemplate (PEG-PEI-rGO) based on PEI and PEG and demonstrated its enhanced photothermally triggered cytosolic drug delivery of DOX [151]. Li et al. developed a unique strategy based on GO to dissociate amyloid aggregation which is beneficial in the treatment of Alzheimer's disease [152]. This was observed by using thioflavin-S (ThS)-modified GO to generate heat for the dissociation of amyloid. All these findings highlight the necessity of careful material design to achieve better dispersity and stability of graphene-related materials with the ultimate goal of achieving higher PT efficiency.

2D BP also has unique properties to determine its applicability in PTT. One of the drawbacks of BP is its intrinsic instability due to the high reactivity of oxygen and water, hindering its applications. Several efforts have been employed to tackle this issue, and surface modification appears to be among the best to enhance the PT performances of bare BP. In a pioneering work by Mei and coworkers, polydopamine (PDA) modification was applied on bare BP to synthesize a novel multifunctional co-delivery system for targeted gene/chemo/PTT [153]. Briefly, permeability glycoprotein siRNA (P-gp siRNA) was adsorbed to the surface of BP, followed by DOX loading. Then, that system was grafted by PDA followed by decorating with an aptamer (NH_2-PEG-Apt) to achieve active tumor targeting capacity while providing excellent physiological stability. PDA-modified BP showed enhanced PT activity based on temperature changes upon NIR laser irradiation. Incredibly, there was a minimum indication of degradation of PT performances even after 3 days exhibited by PT heating curves. Additionally, the hybrid system was beneficial in targeted chemo and gene delivery. Zhao et al. introduced Nile Blue dye to BP (NB@BPs) through diazonium chemistry and found that surface-modified BP exhibit NIR fluorescence enabling NIR imaging-guided PTT [62]. NB@BPs and BP shows temperature rise of 23.5 and 11.5 °C confirming the superiority of NB@BPs as an efficient PT agent. This is further confirmed by shrink and complete tumor removal after 16 days [Fig. 6(c), (d)]. Mice with MCF7 cancer cells were used with 808 nm laser irradiation to evaluate the PT performances. On the other hand, integrating BP with different nanomaterials has become an attractive strategy to achieve satisfactory treatment. Inspired by that Hu and coworkers harvested a nanocomposite by integrating AuNPs, polypyrrole (PPy), and PEG with BP sheets (Au-BPS-PPy-PEG), illustrating excellent PT conversion efficiency and simultaneously improvement of reactive oxygen species (ROS) generation [23]. Here, higher ROS generation was attributed to the creation of Schottky barriers to inhibit electron recombination after incorporating Au, which is highly beneficial in sonodynamic cancer therapy. Additionally, the hybrid nanocomposite is benefited from the superior PT efficiency provided by PPy. Additional methods including atomic layer deposition of Al_2O_3, [154] SiO_2 passivation [155], encapsulation with graphene and BN [156], coordination with titanium sulfonate ligand [157], Te doping [158], and edge selective functionalization with C_{60} molecules [159] have been proven to slow down the reactivity of BP toward oxygen and water.

MXenes structure is endowed with remarkable properties which are applicable in PTT. MXenes are hydrophilic and have strong absorption in the NIR region, opening a wide door for studies in cancer therapy applications. For example, Ti_3C_2, Nb_2C, and Ta_4C_3 have demonstrated in PTT with significantly high PT conversion efficiencies of 30.6, 36.5, and 34.9%, respectively [24, 109, 115]. Schematic illustration of the theranostic capability of Ti_3C_2-based nanocomposite is depicted in Fig. 6(b). In a demonstration by Wu and colleagues, manganese oxide NP-decorated Ti_3C_2 for multiple imaging-guided PT hyperthermia of cancer was reported [77]. The presence of high atomic number Ta is beneficial in X-ray/CT contrast for CT imaging while manganese oxide NPs exhibited unique T_1-weighted MR imaging capability ensuring efficient tumor ablation. Infrared thermal imaging showed a temperature increase to 55 °C in 4T1 breast tumor-bearing mice injected with nanocomposite which is sufficient for tumor ablation [Fig. 6(f)]. On the other hand, mice injected without nanocomposite only showed temperature increase by 5 °C further demonstrating therapeutic efficiency of the nanocomposite. Schematic representation of the theranostic functions of the composite nanosheets is shown in Fig. 6(a). Au, silver (Ag), and other metallic NPs are characterized by localized surface plasmon resonance (LSPR) that have great potential in building heterostructures for PT applications [160–162]. To

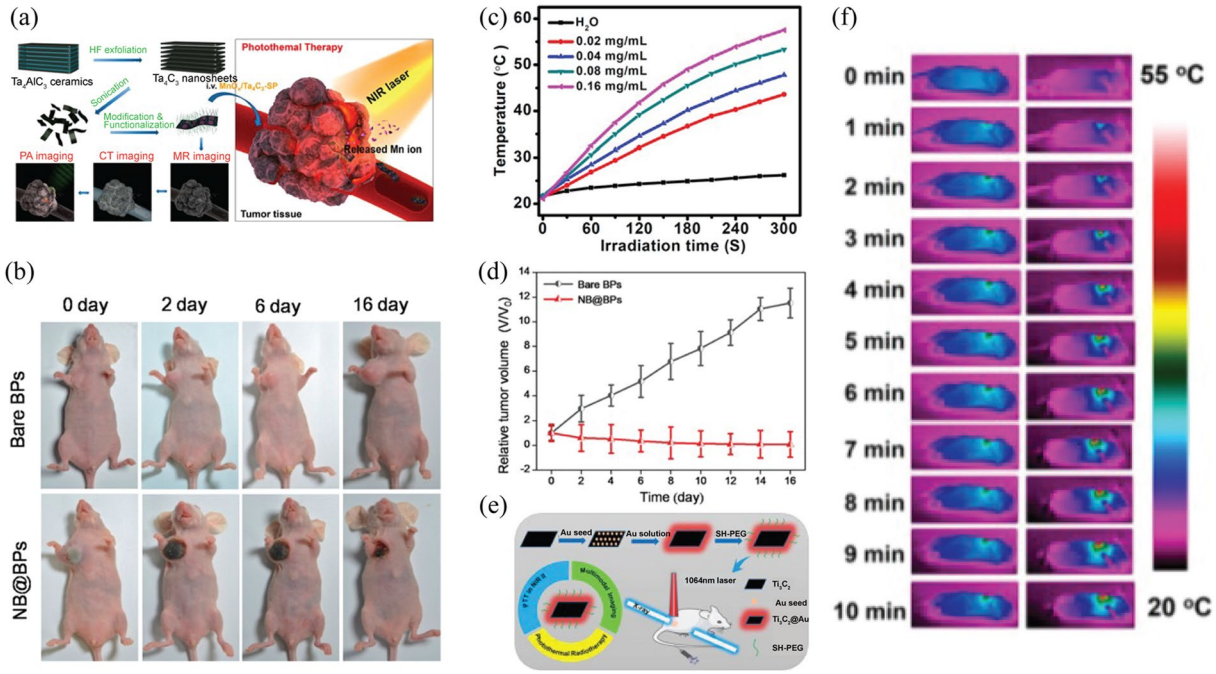

Figure 6: Various applications of 2D materials in PTT. (a) Schematic illustration of synthesis and theranostic functions of MnO_x/Ta_4C_3–SP composite nanosheets. Adapted with permission from Reference [77] © 2017 American Chemical Society. (b) PT heating curves of pure water and Ti_3C_2@Au nanocomposites with various concentrations. Adapted with permission from Reference [76] © 2019 American Chemical Society. (c) Typical photograph and (d) Tumor growth curves of the MCF7 breast tumor-bearing nude mice irradiated by the 808 nm and 1.5 W cm^{-2} NIR laser for 10 min after intravenous injection of bare BPs and NB@BPs. Adapted with permission from Reference [62] © 2017 American Chemical Society. (e) Schematic illustration of the theranostic function of Ti_3C_2@Au. Adapted with permission from Reference [76] © 2017 American Chemical Society. (f) IR thermal images of 4T1 tumor-bearing nude mice with or without intravenous injection of MnO_x/Ta_4C_3–SP nanosheets. Adapted with permission from Reference [77] © 2017 American Chemical Society.

this end, Tang et al. designed multifunctional core–shell nanocomposite based on AuNPs and Ti_3C_2 nanosheets with excellent optical absorption in the NIR region for enhanced PTT therapy in the NIR-I and NIR-II biological windows [Fig. 6(e)] [76]. Here Au was grown on the surface of Ti_3C_2, ensuring stability and biocompatibility of the nanocomposite and higher optical absorbance in NIR-I and NIR-II biological windows. Upon irradiation of 1064 nm laser, the nanocomposite showed concentration-dependent temperature rise, as shown on PT heating curves of Fig. 6b. Additionally, high optical absorbance and strong X-ray attenuation ability played a critical role in PA and CT dual-mode imaging. Motivated by that, Zhu et al. developed a Ti_3C_2-based nanocomposite ($Ti_3C_2T_x$-Pt-PEG) with the aid of Pt NPs for phototheranostics applications [75]. These examples reveal some of the approaches taken by scientists to maximize the potential of MXenes, such as surface functionalization, and use them in multimodal therapies.

2D TMDs are another promising layered material with favorable properties in PTT. Biocompatible-PEGylated WS_2 nanosheets were synthesized through a thiol chemistry method that was highly stable in physiological solutions with no observable toxicity [17]. Furthermore, the authors reported that functionalized nanosheets show promising results as bimodal contrast agents for CT and PAT imaging. Additionally, PEGylated MoS_2 nanosheets possess a strong NIR absorbance and potent in vitro PTT efficiency. In another report, Wang et al. presented hyperbranched polyglycidyl (HPG)-modified MoS_2 (MoS_2–HPG) to use them in combined chemo-PTT [163]. PT performance of MoS_2–HPG was tested, illustrating an increase in the temperature of 34 °C upon NIR light irradiation, and PT conversion efficiency was found to be 29.4%. These examples demonstrate 2D TMDs as effective platform for cancer treatment therapies.

Tissue engineering

Tissue engineering has emerged as a popular pathway to repair and regenerate damaged tissues using biocompatible engineering materials. Scaffolds created from nature-based materials and biopolymers have been utilized in the past due to their biocompatibility, but they have poor mechanical strength and degrade much faster [27]. 2D materials have emerged as potential candidates for tissue engineering applications in the past few years due to their unique physicochemical properties, biocompatibility, biodegradability, low cellular toxicity, and large surface area. These excellent properties have led to the utilization of these

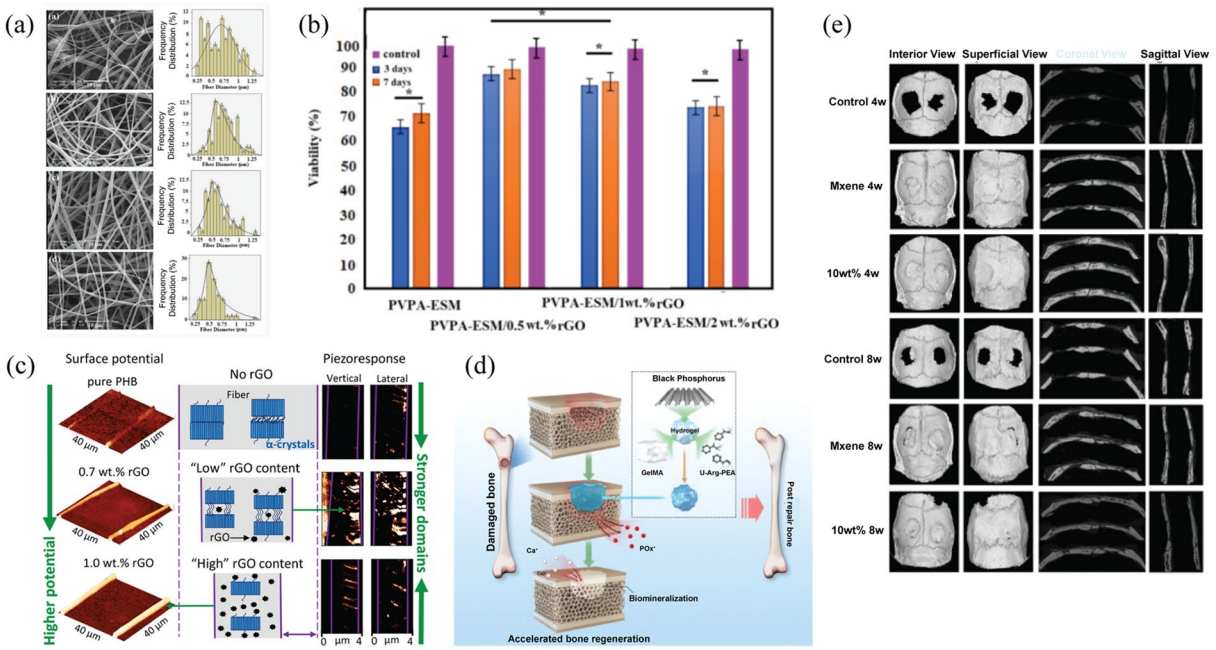

Figure 7: Various tissue engineering applications in 2D materials. (a) Scanning electron microscopy images and frequency distribution of the fiber diameter for PVPA–ESM composites with no rGO, 0.5 wt% rGO, 1 wt% rGO, and 2 wt% rGO fibers, respectively. Adapted with permission from Reference [164] © 2021 MDPI. (b) Cell viability of PVPA–ESM/x wt% rGO nanofibers with various rGO concentrations ($x = 0$, 0.5, 1 ,and 2 wt%). Adapted with permission from Reference [164] © 2021 MDPI. (c) Surface potential distribution from KFPM for PHB and PHB-rGO single fibers on the surface of ITO-PET substrates. Vertical and lateral PFM images of the fibers. Adapted with permission from Reference [165] © 2021 Elsevier. (d) Schematic showing the BP nanosheet based 3D hydrogel scaffold for effective bone regeneration. Adapted with permission from Reference [169] © 2019 American Chemical Society. (e) CT scan images showing bone regeneration performance in the control group, MXene group and HA/MXene group at 4 and 8 weeks after surgery. Adapted with permission from Reference [173] © 2021 Elsevier.

materials as scaffolds for bone tissue, cardiac tissue, neural tissue, skin tissue, and skeletal muscle regeneration [29].

Surface morphology plays a vital role in the biocompatibility of a material and its potential use as biomaterials. Graphene and its derivatives like GO and rGO are crucial due to the presence of wrinkles on their surface, which increases the surface roughness allowing cells to attach to them easily [28]. The oxygen functional groups on GO can lead to the generation of oxidative stress, which destroys the outer cell membrane of *E. coli* [14]. Meanwhile, rGO showed higher antibacterial properties than GO due to its higher electrical conductivity. In both cases, the sharp edges of the nanosheets were thought to contribute to membrane stress which enhanced the antibacterial effect [14].

An effective way to prevent infection and heal wounds is by using biocompatible scaffolds with tissue regenerative capabilities. Sheish et al. used the electrospinning method to synthesize polyvinylpyrrolidone-acrylic acid hydrogel (PVPA)–eggshell membrane (ESM) nanocomposites with different weight percentages of rGO nanosheets, as shown in Fig. 7(a) [164]. The rGO reduced the fiber diameter and increased the water permeability of fibers, which helped enhance the composite's water swelling ratio and biodegradability. The composite wound dressing with rGO also increased the PC12 cell viability compared to non rGO loaded PVPA-ESM nanofiber wound dressing, as shown in Fig. 7(b) [164].

Piezoelectricity is being considered as an essential functionality for bone tissue engineering; however, there are challenges with synthesizing biocompatible piezoelectric materials. Recently, rGO-based hybrid biomaterial scaffolds utilizing biodegradable poly(3-hydroxybutyrate) (PHB) have been reported with enhanced piezoresponse and surface electric potential [165]. The surface potential of the PHB fibers increased with increasing the rGO content to 1 wt%, and 2.5 times increased out-of-plane piezoresponse was observed for PHB fibers with rGO, as depicted in Fig. 7(c). GO can form a functional neural network with an enhanced degree of neural differentiation and regeneration [166]. GO has also been used as a candidate for cardiac tissue engineering due to the similarity between its electrical and mechanical properties with natural cardiac tissue [15]. Choe et al. developed encapsulated mesenchymal stem cells (MSC) with GO and alginate microgels as promising materials for repairing heart tissues after myocardial infarction [167]. These examples highlight the various ways in which scientists have engineered GO and rGO-based nanocomposites for tissue engineering applications.

BP is an exciting material for tissue engineering due to its chemical composition. Phosphorous is a naturally occurring

element that is very important in bone tissue regeneration in the human body in the form of phosphate ions; therefore, BP is highly biocompatible [168]. Even its degradation in the human body leads to the slow release of phosphate ions which contribute to bone regeneration. This property has been utilized to create BP nanosheets-based 3D hydrogel scaffolds that act as a stable source of phosphorous ions without any external calcium ions, thus promoting bone tissue growth [Fig. 7(d)] [169]. The hydrogel was synthesized using cross-linked gelatin methacrylamide, BP nanosheets, and cationic arginine-based unsaturated polyester amides, providing mechanical strength and capturing the released calcium ions, thus accelerating biomineralization. Rauchi et al. used exfoliated few-layer BP to study its impact on bone regeneration [64]. They used an in vitro model and found that BP stimulates bone tissue growth after an osteosarcoma resection by promoting the growth and osteogenic differentiation of human preosteoblast (Hob) and mesenchymal stem cells. 2D BP has also increased the anti-inflammatory interleukin-10 generation and inhibited the pro-inflammatory interleukin-6 synthesis. Bioinspired matrix vesicles have also been synthesized with BP QDs to stimulate bone mineralization [170]. Matrix vesicles are a type of extracellular vesicles that regulate bone mineralization. BP, in this case, provides the inorganic phosphate ions and shows a PT effect displaying outstanding bone regeneration performance. BP has emerged as an excellent candidate for tissue engineering applications due to its high loading efficiency, excellent biocompatibility, and noncytotoxic degradation into phosphate ions.

MXenes are 2D inorganic compounds of which first reported use for tissue engineering came in 2011 when Annunziata et al. studied the effect of titanium nitride (TiN) coating on titanium plasma-sprayed (TPS) dental implant surfaces. The TiN coating increased the physio-mechanical properties and the esthetics of the implant while simultaneously reducing the adhesion and growth of oral bacterial cultures [171]. TiC bone implants have also been explored to improve bone osteointegration in rabbit femurs in an in vivo experiment [172]. Fu et al. studied the use of 2D TiC nanosheets-hydroxyapatite (HA) nanowires composite membrane as potential materials for bone regeneration [173]. The ultralong HA nanowires could easily interact with TiC due to its surface terminated functional groups, including fluorine and oxygen, enhancing their combination through hydrogen bonding. The nanocomposite exhibited unique surface topography with improved mechanical properties and hydrophilicity, increasing its biocompatibility and osteogenic differentiation ability. The nanocomposite was also put to clinical use in a rat calvarial bone defect where it effectively enhanced bone tissue generation [Fig. 7(e)] and thus can be potentially used in dental applications.

TMDs, especially MoS_2, have also been utilized in biomaterial applications due to their good cellular compatibility and sizeable specific area. MoS_2-polyacrylonitrile (PAN) composite nanofibers have been prepared using electrospinning combined with a doping method displaying great biocompatibility [174]. The nanofibers composites promoted the growth of bone-marrow mesenchymal stem cells while maintaining their cellular activity and proliferation. MoS_2 composite nanosheets have also been utilized as a conductive scaffold for cardiac tissue engineering [175]. Nazari et al. prepared electrospun MoS_2 nanosheets and nylon 6 nanocomposite scaffolds which showed enhanced cellular attachment, cell proliferation, and cardiogenic differentiation in mouse embryonic cardiac cells [175]. Despite their applications, there are concerns about cytotoxicity and slow degradation of MoS_2 due to its crystalline nature, limiting its potential for clinical use.

2D h-BN is an insulator material with robust inertness and thermal stability, enabling its use in many biomedical applications. It has been used to prepare sintered h-BN-HA composites derived from bovine bones with up to 1.5 wt% h-BN [176]. The presence of h-BN in the composite led to a fine crystalline microstructure with good mechanical properties. Biological testing of the h-BN-HA composite showed no adverse effects on human bone osteosarcoma proliferation while also showing antibacterial activity against *Enterococcus faecalis* bacteria. Thus, all the recent studies highlighted above indicate the potential use of 2D material-based scaffolds and other hybrid structures for tissue engineering applications.

Emerging role of machine learning toward 2D material-based biomedical applications

In recent years, ML is thriving in the fields of bioimaging, biosensing as well as other biomedical applications [16, 177–179]. ML algorithms including support vector machine (SVM), random forest (RF), convolutional neural network (CNN), etc. have been applied to various biosensing data analyses and can be easily extended to 2D material-based biomedical applications [Fig. 8(a) and (b)]. The most common application that ML methods are used in bioimaging and biosensing is classifying target analyte categories [16]. For example, ML classification of MRI images has been used to diagnose Alzheimer's disease [180], brain cancer [181], heart disease [182], etc. Recently, Isamel et al. utilized CNN to classify 3 brain tumor types (Meningiomas, Gliomas, and Pituitary tumors) with MRI images [181]. They used ResNet50 and achieved 99% accuracy which is a state-of-the-art result that outperformed all previous works [183]. CT images have a similar data type and can also be fed into ML to detect cancers [184], viruses [185], etc. With the combination of ML and CT images, Barstugan et al. diagnosed COVID-19 disease and obtained 99% accuracy using the SVM classifier [186]. A recent study by Ye et al. used various ML models to classify respiratory viruses based on Raman-sensing data

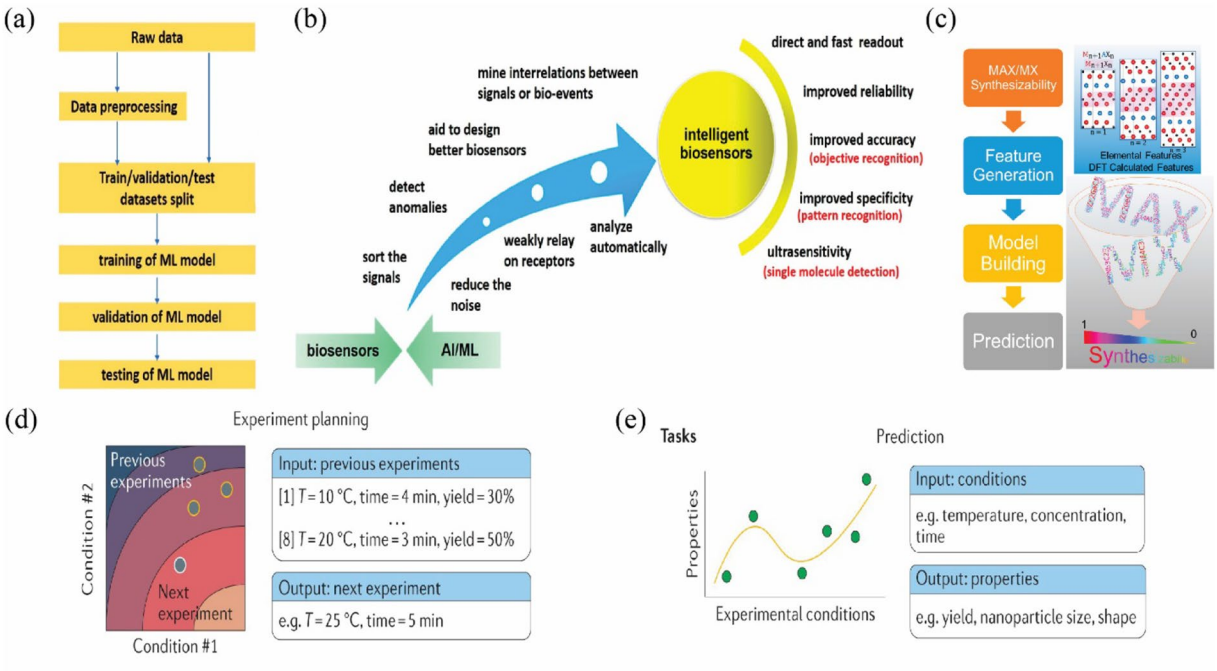

Figure 8: Illustration of applicability of ML in materials science and biomedical applications. (a) General process of ML-based data analysis. Adapted with permission from Reference [16] © 2020 American Chemical Society. (b) Benefits of ML brought to biosensors. Adapted with permission from Reference [16] © 2020 American Chemical Society. (c) Structural models of bulk MAX phase (upper right) and the corresponding MXene highlighted in pinks. Word clouds (lower right) where large (small) font size and red (orange) color correspond to high (low) predicted synthesizability of the named compound. Adapted with permission from Ref. [189] © 2019 American Chemical Society. (d) ML tasks in NP synthesis. In predictions tasks, ML predicts NP properties based on experimental conditions. Adapted with permission from Ref. [190] © 2021 Springer Nature Limited. (e) In experiment-planning tasks, ML proposes new experiments to find an optimal set of conditions that result in NP with the desired properties. Adapted with permission from Ref. [190] © 2021 Springer Nature Limited.

[187]. In addition, interpretable ML has been applied to understanding Alzheimer's disease biomarkers based on 2D material-assisted Raman spectroscopy [120]. ML has greatly accelerated the analyses of different types of biosensing data. The merits of advanced ML assistance on biosensing can also be directly extended to other 2D material-based biomedical applications.

Besides the outstanding performance in bioimaging and biosensing, ML approaches are also prospering in 2D material design, especially synthesis condition prediction which can boost biomedical applications [188]. Recently, Frey et al. used a positive and unlabeled ML algorithm and achieved prediction of synthesis of 2D metal carbides and nitrides [189]. They designed a deep neural network and identified 18 MXene compounds to be promising for synthesis, which are emerging materials for biomedical applications [Fig. 8(c)] [3]. Researchers can also utilize heuristic ML algorithms such as the genetic algorithm to design experiments of 2D martial synthesis. However, this area is still novel and lacks fundamental studies. Although there are limited resources on 2D material design with ML, a considerable amount of work on NP design can be directly transferred by simply applying relevant datasets without modifying the algorithm [190]. A heuristic strategy-based algorithm named stable noisy optimization by branch and fit (SNOBFIT) is frequently used to guide NP synthesis experiment design [Fig. 8(d)] [191]. For example, SNOBFIT can provide unexplored growth temperature that can possibly result in the desired height of peaks in nanoparticle spectra by building linear and quadratic models that capture the correlation between previous growth temperatures and outcome intensity of emission wavelength [192, 193]. Additionally, to facilitate efficient material design for biomedical applications, ML can predict the target material by configuring desired electronic properties, thermal conductivity, and optical properties (Fig. 8e) [194]. For example, Sun et al. used artificial neural networks to analyze Ag nanoparticles by mapping Fermi energy onto geometrical, structural, topological, and morphological features [195]. Again, these techniques can be applied to 2D material and related studies are required in the future. With ML-assisted synthesis condition prediction, synthesis experiment design, and material property configuration, researchers can easily find proper materials for different biomedical applications.

ML is a promising tool that is essential in both biosensing analyses and biosensing-related 2D material design. There are existing techniques in biosensing that can be directly applied to 2D material-based biosensing. For 2D materials design in biomedical applications, there are also thorough studies on synthesis prediction. As potential future prospective directions, ML-assisted

2D material synthesis experiment design and material property configuration can be developed based on ML-assisted nanoparticle studies.

Conclusion and prospects

In this article, state-of-the-art research works based on 2D-layered materials designed for biomedical applications have been systematically reviewed with a strong focus on surface engineering and benchmark biomedical applications. Graphene and other layered materials bring exciting new opportunities in biomedical applications such as drug delivery, cancer therapy, gene delivery, bioimaging, etc. The most fascinating feature of these layered materials is integrating multiple functions into a nanodevice to facilitate research and development. A variety of structural and surface engineering methods have been developed to manipulate properties of 2D-layered materials while maintaining their biocompatibility for expanding biomedical applications. Strain engineering and folding are the main 2D material structural-engineering paths allowing manipulation of optoelectronic properties. Defect engineering is proved to be an effective way for improving and modulating the biomedical performance of 2D-layered materials. Engineering approaches such as e-beam/ion/laser irradiation, plasma treatment, and substitutional doping have been utilized to introduce defects in the materials. Although great progress has been made in the past decades, many challenges and obstacles lack the investigation of 2D materials-based biomedical applications. First, there is an absence of a comprehensive understanding of the correlation between atomic-scale defects and optical or electronic properties of the materials. Second, introducing defects with precise control in distribution and density is still not yet achieved experimentally. Furthermore, characterization techniques and calculation interpretation are still evolving, which are also essential in utilizing defects in biomedical applications.

Engineering of 2D materials, including the application of strain and assembling of various 2D materials into heterostructures, has been the key technology to manipulate structural properties. Application of strain in 2D materials provides a new degree of freedom of electronic band structure tuning, creating novel and exotic optical or electrical properties, which can be utilized in biomedical device design. 2D heterostructures enable another way to tailor material properties, leading to the design of better performing optical/electrical/biomedical nanodevices. Additionally, 2D materials can offer an easy and effective way of addressing the need for better device fabrication for biomedical applications by considering band alignments. A recent report suggested 2D vdWs heterostructures based on different band alignments are beneficial for a series of biomedical applications [196]. For example, BP-WSe_2 heterostructure, which follows the type-I band arrangement, allows the transfer of electrons and holes from one material to another. This results in enhanced radiative recombination of carriers suitable for fluorescence bioimaging. They prepared WSe_2/BP/WSe_2 heterostructure after chemical treatment and surface modification. More importantly, the proposed heterostructure can emit NIR radiation and generates heat which is applicable in PTT. On the other hand, they proposed MoS_2/WSe_2 heterostructure with type-II band arrangement for cancer treatments benefiting from strong IR absorption and drug delivery applications. Therefore, the preparation of different 2D materials heterostructures satisfying type-I and type-II band arrangement could open a world of opportunities to revolutionize medical strategies.

As surface functionalization provides great inspiration for scientists to develop materials for a range of applications, there should be continuous efforts dedicated to assembling 2D materials with NPs and QDs for clinical translation. Emerging functionalization strategies such as intercalation by metallic atoms or molecules should receive more attention as it is a great way to modify the band structure of 2D materials. One of the main obstacles in clinical transformation is the non-specific binding of non-target molecules toward biosensors which interferes with the accurate determination of the limit of detection. Therefore, developing functionalization strategies that inhibit non-specific binding is highly demanding. Another potential direction would be 2D material optical sensors based on SPR as a label-free technique for the rapid diagnosis of diseases. In this regard, attention should be oriented toward better sensor design with enhanced sensitivity, specificity, and reproducibility of detection.

In parallel to developing better surface and structural-engineering platforms that respond to modern-day health care needs, this field needs to dive into ML approaches that can help understand and optimize 2D material synthesis pathways. Such methods will allow scientists in academia and industry to efficiently design 2D materials by avoiding time and cost associated with traditional empirical trial and error methods and the density functional theory. As toxicity is one of the barriers to using 2D materials in healthcare applications, ML approaches can be employed to study 2D material toxicity [197–200]. Additionally, there is a great capacity to use ML-assisted 2D material synthesis to explore structure–property relationships. Unlocking the true potential of ML in 2D material synthesis and corresponding applications will require concerted efforts from a broader community, as discussed in the article. We anticipate that realization of ML-assisted 2D material discovery would be a revolutionary step in transforming these materials into biomedical applications.

So far, remarkable progress and excellent future opportunities are evident in this field while highlighting the growing need for better device fabrication and cost-effective manufacturing processes. The full utilization of 2D materials in clinical applications still requires ongoing efforts as the development of

2D materials for biomedical applications is still in its immature stage. For instance, the development of large-scale synthesis and engineering approaches to prepare layered materials with the highest purity while maintaining their size, shape, and charge is of paramount importance to achieve sensitive and controllable biosensing platforms. Additionally, research into new avenues of nanoscale optical engineering is expected to boost 2D material-based biomedical applications. Integrating materials science with computational approaches such as ML is a prerequisite to responding to the needs of modern healthcare applications. On the other hand, a better understanding of the biological behavior of 2D material inside living bodies is largely unknown, which presents a significant barrier in clinical applications. Therefore, substantial efforts should be aimed toward biosafety assessment with animal models to gain an in-depth understanding of immunomodulation, pharmacodynamics, and pharmacokinetic profiles of 2D nanomaterials and their heterostructures. This will enable the active targeting ability of 2D material-based theranostic agents. In order to have a competitive advantage over traditionally used nanocomposites, the commercialization of 2D materials faces another hurdle. Such limitations can be overcome by exploring the mass production of high-quality 2D materials. These developments are expected to lead to personalized medicine that can fill voids in modern health care through collaborations involving materials science, biomedical engineering, chemistry, and emerging ML pathways. The recent COVID-19 pandemic alerts us that better access to disease prevention, diagnosis, and treatment is highly demanded. In this regard, engineered 2D materials hold great promise in new sensing modalities that significant impact on medical diagnosis. Thus, exploring new avenues of 2D material-based biomedical applications will unlock the true potential of personalized medicine. Overall, the rapid development of materials science and ML capabilities is continuously pushing the boundaries of 2D materials-based biosensing and biomedical applications. We hope this review will open a new avenue to this burgeoning field.

Acknowledgments

This work is financially supported by Johnson & Johnson Inc. for the STEM2D Scholar's Award and National Science Foundation CAREER Award Grant Number ECCS-1943895, EArly-concept Grants for Exploratory Research (EAGER) Grant number 2030857, and Growing Convergence Research (GCR) Grant number ECCS-1934977.

Data availability

Data sharing not applicable to this article as no datasets were generated or analyzed during the current study.

Declarations

Conflict of interest The authors declare that they have no known competing financial interests or personal relationships that could have appeared to influence the work reported in this paper.

References

1. J.R. Choi, K.W. Yong, J.Y. Choi, A. Nilghaz, Y. Lin, J. Xu, X. Lu, Black phosphorus and its biomedical applications. Theranostics **8**(4), 1005 (2018)
2. X. Ling, H. Wang, S. Huang, F. Xia, M.S. Dresselhaus, The renaissance of black phosphorus. Proc. Natl. Acad. Sci. USA **112**(15), 4523 (2015)
3. A. Sinha, H. Zhao, Y. Huang, X. Lu, J. Chen, R. Jain, MXene: An emerging material for sensing and biosensing. TrAC Trends Anal. Chem. **105**, 424 (2018)
4. B. Xu, C. Zhi, P. Shi, Latest advances in MXene biosensors. J. Phys. Mater. **3**(3), 031001 (2020)
5. K.S. Novoselov, A.K. Geim, S.V. Morozov, D. Jiang, Y. Zhang, S.V. Dubonos, I.V. Grigorieva, A.A. Firsov, Electric field effect in atomically thin carbon films. Science **306**(5696), 666 (2004)
6. A.K. Geim, K.S. Novoselov, The rise of graphene, *in Nanoscience and Technology: A Collection of Reviews from Nature Journals*, (World Scientific, City, 2010), p. 11
7. K.S. Novoselov, D. Jiang, F. Schedin, T. Booth, V. Khotkevich, S. Morozov, A.K. Geim, Two-dimensional atomic crystals. Proc. Natl. Acad. Sci. USA **102**(30), 10451 (2005)
8. S.Z. Butler, S.M. Hollen, L. Cao, Y. Cui, J.A. Gupta, H.R. Gutiérrez, T.F. Heinz, S.S. Hong, J. Huang, A.F. Ismach, Progress, challenges, and opportunities in two-dimensional materials beyond graphene. ACS Nano **7**(4), 2898 (2013)
9. P.K. Kannan, D.J. Late, H. Morgan, C.S. Rout, Recent developments in 2D layered inorganic nanomaterials for sensing. Nanoscale **7**(32), 13293 (2015)
10. X. Zhu, Y. Zhang, M. Liu, Y. Liu, 2D titanium carbide MXenes as emerging optical biosensing platforms. Biosens. Bioelectron. **171**, 112730 (2021)
11. G. Yang, H. Gong, T. Liu, X. Sun, L. Cheng, Z. Liu, Two-dimensional magnetic WS_2@ Fe_3O_4 nanocomposite with mesoporous silica coating for drug delivery and imaging-guided therapy of cancer. Biomaterials **60**, 62 (2015)
12. A. Rebekah, S. Sivaselvam, C. Viswanathan, D. Prabhu, R. Gautam, N. Ponpandian, Magnetic nanoparticle-decorated graphene oxide-chitosan composite as an efficient nanocarrier for protein delivery. Colloid Surf. A **610**, 125913 (2021)
13. Z. Liu, M. Zhao, H. Lin, C. Dai, C. Ren, S. Zhang, W. Peng, Y. Chen, 2D magnetic titanium carbide MXene for cancer theranostics. J. Mater. Chem. B **6**(21), 3541 (2018)

14. S. Liu, T.H. Zeng, M. Hofmann, E. Burcombe, J. Wei, R. Jiang, J. Kong, Y. Chen, Antibacterial activity of graphite, graphite oxide, graphene oxide, and reduced graphene oxide: membrane and oxidative stress. ACS Nano **5**(9), 6971 (2011)
15. J. Lee, V. Manoharan, L. Cheung, S. Lee, B.-H. Cha, P. Newman, R. Farzad, S. Mehrotra, K. Zhang, F. Khan, Nanoparticle-based hybrid scaffolds for deciphering the role of multimodal cues in cardiac tissue engineering. ACS Nano **13**(11), 12525 (2019)
16. F. Cui, Y. Yue, Y. Zhang, Z. Zhang, H.S. Zhou, Advancing biosensors with machine learning. ACS Sens. **5**(11), 3346 (2020)
17. L. Cheng, J. Liu, X. Gu, H. Gong, X. Shi, T. Liu, C. Wang, X. Wang, G. Liu, H. Xing, PEGylated WS_2 nanosheets as a multifunctional theranostic agent for in vivo dual-modal CT/photoacoustic imaging guided photothermal therapy. Adv. Mater. **26**(12), 1886 (2014)
18. X. Sun, Z. Liu, K. Welsher, J.T. Robinson, A. Goodwin, S. Zaric, H. Dai, Nano-graphene oxide for cellular imaging and drug delivery. Nano Res. **1**(3), 203 (2008)
19. Q. Xue, H. Zhang, M. Zhu, Z. Pei, H. Li, Z. Wang, Y. Huang, Y. Huang, Q. Deng, J. Zhou, Photoluminescent Ti_3C_2 MXene quantum dots for multicolor cellular imaging. Adv. Mater. **29**(15), 1604847 (2017)
20. H. Bao, Y. Pan, Y. Ping, N.G. Sahoo, T. Wu, L. Li, J. Li, L.H. Gan, Chitosan-functionalized graphene oxide as a nanocarrier for drug and gene delivery. Small **7**(11), 1569 (2011)
21. S. Goenka, V. Sant, S. Sant, Graphene-based nanomaterials for drug delivery and tissue engineering. J. Control. Releas. **173**, 75 (2014)
22. J. Liu, L. Cui, D. Losic, Graphene and graphene oxide as new nanocarriers for drug delivery applications. Acta Biomater. **9**(12), 9243 (2013)
23. W. Chen, J. Wang, W. Du, J. Wang, L. Cheng, Z. Ge, S. Qiu, W. Pan, L. Song, X. Ma, Black phosphorus nanosheets integrated with gold nanoparticles and polypyrrole for synergistic sonodynamic and photothermal cancer therapy. ACS Appl. Nano Mater. **4**(8), 7963 (2021)
24. H. Lin, X. Wang, L. Yu, Y. Chen, J. Shi, Two-dimensional ultrathin MXene ceramic nanosheets for photothermal conversion. Nano Lett. **17**(1), 384 (2017)
25. T. Liu, Y. Chao, M. Gao, C. Liang, Q. Chen, G. Song, L. Cheng, Z. Liu, Ultra-small MoS_2 nanodots with rapid body clearance for photothermal cancer therapy. Nano Res. **9**(10), 3003 (2016)
26. J.T. Robinson, S.M. Tabakman, Y. Liang, H. Wang, H. Sanchez Casalongue, D. Vinh, H. Dai, Ultrasmall reduced graphene oxide with high near-infrared absorbance for photothermal therapy. J. Am. Chem. Soc. **133**(17), 6825 (2011)
27. J.R. Gershlak, S. Hernandez, G. Fontana, L.R. Perreault, K.J. Hansen, S.A. Larson, B.Y. Binder, D.M. Dolivo, T. Yang, T. Dominko, Crossing kingdoms: Using decellularized plants as perfusable tissue engineering scaffolds. Biomaterials **125**, 13 (2017)
28. J. Zhang, H. Chen, M. Zhao, G. Liu, J. Wu, 2D nanomaterials for tissue engineering application. Nano Res. **13**(8), 2019 (2020)
29. Y. Zheng, X. Hong, J. Wang, L. Feng, T. Fan, R. Guo, H. Zhang, 2D nanomaterials for tissue engineering and regenerative nanomedicines: recent advances and future challenges. Adv. Healthc. Mater. **10**(7), 2001743 (2021)
30. S. Bertolazzi, J. Brivio, A. Kis, Stretching and breaking of ultrathin MoS_2. ACS Nano **5**(12), 9703 (2011)
31. A. Silver, H. Kitadai, H. Liu, T. Granzier-Nakajima, M. Terrones, X. Ling, S. Huang, Chemical and bio sensing using graphene-enhanced Raman spectroscopy. Nanomaterials **9**(4), 516 (2019)
32. J.H. Jung, D.S. Cheon, F. Liu, K.B. Lee, T.S. Seo, A graphene oxide based immuno-biosensor for pathogen detection. Angew. Chem. **122**(33), 5844 (2010)
33. A. Mathkar, D. Tozier, P. Cox, P. Ong, C. Galande, K. Balakrishnan, A. LeelaMohana Reddy, P.M. Ajayan, Controlled, stepwise reduction and band gap manipulation of graphene oxide. J. Phys. Chem. Lett. **3**(8), 986 (2012)
34. P. Sehrawat, S. Islam, P. Mishra, S. Ahmad, Reduced graphene oxide (rGO) based wideband optical sensor and the role of Temperature, Defect States and Quantum Efficiency. Sci. Rep. **8**(1), 1 (2018)
35. L. Li, Y. Yu, G.J. Ye, Q. Ge, X. Ou, H. Wu, D. Feng, X.H. Chen, Y. Zhang, Black phosphorus field-effect transistors. Nat. Nanotechnol. **9**(5), 372 (2014)
36 A. Chaves, J. Azadani, H. Alsalman, D.R. da Costa, R. Frisenda, A. Chaves, S.H. Song, Y. Kim, D. He, J. Zhou, Bandgap engineering of two-dimensional semiconductor materials. NPJ 2D Mater. Appl. **4**(1), 1 (2020)
37. M. Buscema, D.J. Groenendijk, S.I. Blanter, G.A. Steele, H.S. Van Der Zant, A. Castellanos-Gomez, Fast and broadband photoresponse of few-layer black phosphorus field-effect transistors. Nano Lett. **14**(6), 3347 (2014)
38. K. Kam, B. Parkinson, Detailed photocurrent spectroscopy of the semiconducting group VIB transition metal dichalcogenides. J. Phys. Chem. **86**(4), 463 (1982)
39. H.M. Hill, A.F. Rigosi, K.T. Rim, G.W. Flynn, T.F. Heinz, Band alignment in MoS_2/WS_2 transition metal dichalcogenide heterostructures probed by scanning tunneling microscopy and spectroscopy. Nano Lett. **16**(8), 4831 (2016)
40. C. Elias, P. Valvin, T. Pelini, A. Summerfield, C. Mellor, T. Cheng, L. Eaves, C. Foxon, P. Beton, S. Novikov, Direct band-gap crossover in epitaxial monolayer boron nitride. Nat. Commun. **10**(1), 1 (2019)
41. M. Khazaei, A. Ranjbar, M. Arai, T. Sasaki, S. Yunoki, Electronic properties and applications of MXenes: a theoretical review. J. Mater. Chem. C. **5**(10), 2488 (2017)

42. J. Fang, W.G. Vandenberghe, M.V. Fischetti, Microscopic dielectric permittivities of graphene nanoribbons and graphene. Phys. Rev. B. **94**(4), 045318 (2016)
43. E. Prokhorov, Z. Barquera-Bibiano, A. Manzano-Ramírez, G. Luna-Barcenas, Y. Kovalenko, M. Hernández-Landaverde, B.C. Reyes, J.H. Vargas, New insights in graphene oxide dielectric constant. Mater. Res. Express **6**(8), 085622 (2019)
44. P. Kumar, B. Bhadoria, S. Kumar, S. Bhowmick, Y.S. Chauhan, A. Agarwal, Thickness and electric-field-dependent polarizability and dielectric constant in phosphorene. Phys. Rev. B. **93**(19), 195428 (2016)
45 A. Laturia, M.L. Van de Put, W.G. Vandenberghe, Dielectric properties of hexagonal boron nitride and transition metal dichalcogenides: from monolayer to bulk. NPJ 2D Mater. Appl. **2**(1), 1 (2018)
46. G. Berdiyorov, Optical properties of functionalized $Ti_3C_2T_2$ (T= F, O, OH) MXene: first-principles calculations. AIP Adv. **6**(5), 055105 (2016)
47. K.I. Bolotin, K.J. Sikes, Z. Jiang, M. Klima, G. Fudenberg, J. Hone, P. Kim, H. Stormer, Ultrahigh electron mobility in suspended graphene. Solid State Commun. **146**(9–10), 351 (2008)
48. S. Ahmed, J. Yi, Two-dimensional transition metal dichalcogenides and their charge carrier mobilities in field-effect transistors. Nano-Micro Lett. **9**(4), 1 (2017)
49. H. Zhang, G. Yang, X. Zuo, H. Tang, Q. Yang, G. Li, Computational studies on the structural, electronic and optical properties of graphene-like MXenes (M_2CT_2, M= Ti, Zr, Hf; T= O, F, OH) and their potential applications as visible-light driven photocatalysts. J. Mater. Chem. A **4**(33), 12913 (2016)
50. N. Briggs, S. Subramanian, Z. Lin, X. Li, X. Zhang, K. Zhang, K. Xiao, D. Geohegan, R. Wallace, L.-Q. Chen, A roadmap for electronic grade 2D materials. 2D Mater. **6**(2), 022001 (2019)
51. K. Kang, S. Xie, L. Huang, Y. Han, P.Y. Huang, K.F. Mak, C.-J. Kim, D. Muller, J. Park, High-mobility three-atom-thick semiconducting films with wafer-scale homogeneity. Nature **520**(7549), 656 (2015)
52. X. Zhang, T.H. Choudhury, M. Chubarov, Y. Xiang, B. Jariwala, F. Zhang, N. Alem, G.-C. Wang, J.A. Robinson, J.M. Redwing, Diffusion-controlled epitaxy of large area coalesced WSe_2 monolayers on sapphire. Nano Lett. **18**(2), 1049 (2018)
53. L.A. Walsh, R. Addou, R.M. Wallace, and C.L. Hinkle, Molecular beam epitaxy of transition metal dichalcogenides, in *Molecular Beam Epitaxy*, (Elsevier, City, 2018), p. 515
54. J. Kim, H. Park, J.B. Hannon, S.W. Bedell, K. Fogel, D.K. Sadana, C. Dimitrakopoulos, Layer-resolved graphene transfer via engineered strain layers. Science **342**(6160), 833 (2013)
55. J.-Y. Moon, M. Kim, S.-I. Kim, S. Xu, J.-H. Choi, D. Whang, K. Watanabe, T. Taniguchi, D.S. Park, J. Seo, Layer-engineered large-area exfoliation of graphene. Sci. Adv. **6**(44), eabc6601 (2020)
56. F. Liu, W. Wu, Y. Bai, S.H. Chae, Q. Li, J. Wang, J. Hone, X.-Y. Zhu, Disassembling 2D van der Waals crystals into macroscopic monolayers and reassembling into artificial lattices. Science **367**(6480), 903 (2020)
57. M. Liu, H. Zhu, Y. Wang, C. Sevencan, B.L. Li, Functionalized MoS_2-based nanomaterials for cancer phototherapy and other biomedical applications. ACS Mater. Lett. **3**(5), 462 (2021)
58. J. Filip, A. Andicsová-Eckstein, A. Vikartovská, J. Tkac, Immobilization of bilirubin oxidase on graphene oxide flakes with different negative charge density for oxygen reduction. The effect of GO charge density on enzyme coverage, electron transfer rate and current density. Biosens. Bioelectron. **89**, 384 (2017)
59. K. Yang, S. Zhang, G. Zhang, X. Sun, S.-T. Lee, Z. Liu, Graphene in mice: ultrahigh in vivo tumor uptake and efficient photothermal therapy. Nano Lett. **10**(9), 3318 (2010)
60. C. Shan, H. Yang, D. Han, Q. Zhang, A. Ivaska, L. Niu, Water-soluble graphene covalently functionalized by biocompatible poly-L-lysine. Langmuir **25**(20), 12030 (2009)
61. W. Zhou, H. Cui, L. Ying, X.F. Yu, Enhanced cytosolic delivery and release of CRISPR/Cas9 by black phosphorus nanosheets for genome editing. Angew. Chem. **130**(32), 10425 (2018)
62. Y. Zhao, L. Tong, Z. Li, N. Yang, H. Fu, L. Wu, H. Cui, W. Zhou, J. Wang, H. Wang, Stable and multifunctional dye-modified black phosphorus nanosheets for near-infrared imaging-guided photothermal therapy. Chem. Mater. **29**(17), 7131 (2017)
63. Z. Li, T. Guo, Y. Hu, Y. Qiu, Y. Liu, H. Wang, Y. Li, X. Chen, J. Song, H. Yang, A Highly effective π–π stacking strategy to modify black phosphorus with aromatic molecules for cancer theranostics. ACS Appl. Mater. Interfaces **11**(10), 9860 (2019)
64. M.G. Raucci, I. Fasolino, M. Caporali, M. Serrano-Ruiz, A. Soriente, M. Peruzzini, L. Ambrosio, Exfoliated black phosphorus promotes in vitro bone regeneration and suppresses osteosarcoma progression through cancer-related inflammation inhibition. ACS Appl. Mater. Interfaces **11**(9), 9333 (2019)
65. L. Wu, J. Wang, J. Lu, D. Liu, N. Yang, H. Huang, P.K. Chu, X.F. Yu, Lanthanide-coordinated black phosphorus. Small **14**(29), 1801405 (2018)
66. G. Qu, W. Liu, Y. Zhao, J. Gao, T. Xia, J. Shi, L. Hu, W. Zhou, J. Gao, H. Wang, Improved biocompatibility of black phosphorus nanosheets by chemical modification. Angew. Chem. Int. Ed. **56**(46), 14488 (2017)
67. Z. Sofer, J. Luxa, D. Bouša, D. Sedmidubský, P. Lazar, T. Hartman, H. Hardtdegen, M. Pumera, The covalent functionalization of layered black phosphorus by nucleophilic reagents. Angew. Chem. Int. Ed. **56**(33), 9891 (2017)
68. V. Kumar, J.R. Brent, M. Shorie, H. Kaur, G. Chadha, A.G. Thomas, E.A. Lewis, A.P. Rooney, L. Nguyen, X.L. Zhong, Nanostructured aptamer-functionalized black phosphorus sensing platform for label-free detection of myoglobin, a

cardiovascular disease biomarker. ACS Appl. Mater. Interfaces. **8**(35), 22860 (2016)

69. S. Wang, K. Li, Y. Chen, H. Chen, M. Ma, J. Feng, Q. Zhao, J. Shi, Biocompatible PEGylated MoS_2 nanosheets: controllable bottom-up synthesis and highly efficient photothermal regression of tumor. Biomaterials **39**, 206 (2015)
70. W. Yin, L. Yan, J. Yu, G. Tian, L. Zhou, X. Zheng, X. Zhang, Y. Yong, J. Li, Z. Gu, High-throughput synthesis of single-layer MoS_2 nanosheets as a near-infrared photothermal-triggered drug delivery for effective cancer therapy. ACS Nano **8**(7), 6922 (2014)
71. Y. Yuan, R. Li, Z. Liu, Establishing water-soluble layered WS_2 nanosheet as a platform for biosensing. Anal. Chem. **86**(7), 3610 (2014)
72. Y. Yong, L. Zhou, Z. Gu, L. Yan, G. Tian, X. Zheng, X. Liu, X. Zhang, J. Shi, W. Cong, WS_2 nanosheet as a new photosensitizer carrier for combined photodynamic and photothermal therapy of cancer cells. Nanoscale **6**(17), 10394 (2014)
73. E. Satheeshkumar, A. Bandyopadhyay, M. Sreedhara, S.K. Pati, C. Rao, M. Yoshimura, One-step simultaneous exfoliation and covalent functionalization of MoS_2 by amino acid induced solution processes. ChemNanoMat. **3**(3), 172 (2017)
74. J. Lee, J. Kim, W.J. Kim, Photothermally controllable cytosolic drug delivery based on core–shell MoS_2-porous silica nanoplates. Chem. Mater. **28**(17), 6417 (2016)
75 Y. Zhu, Z. Wang, R. Zhao, Y. Zhou, L. Feng, S. Gai, P. Yang, Pt decorated $Ti_3C_2T_x$ MXene with NIR-II light amplified nanozyme catalytic activity for efficient phototheranostics. ACS Nano **16**, 3105 (2022)
76. W. Tang, Z. Dong, R. Zhang, X. Yi, K. Yang, M. Jin, C. Yuan, Z. Xiao, Z. Liu, L. Cheng, Multifunctional two-dimensional core–shell MXene@ Gold nanocomposites for enhanced photo–radio combined therapy in the second biological window. ACS Nano **13**(1), 284 (2018)
77. C. Dai, Y. Chen, X. Jing, L. Xiang, D. Yang, H. Lin, Z. Liu, X. Han, R. Wu, Two-dimensional tantalum carbide (MXenes) composite nanosheets for multiple imaging-guided photothermal tumor ablation. ACS Nano **11**(12), 12696 (2017)
78. X. Han, J. Huang, H. Lin, Z. Wang, P. Li, Y. Chen, 2D ultrathin MXene-based drug-delivery nanoplatform for synergistic photothermal ablation and chemotherapy of cancer. Adv. Healthc. Mater. **7**(9), 1701394 (2018)
79. H. Terrones, R. Lv, M. Terrones, M.S. Dresselhaus, The role of defects and doping in 2D graphene sheets and 1D nanoribbons. Rep. Prog. Phys. **75**(6), 062501 (2012)
80. S. Kretschmer, M. Maslov, S. Ghaderzadeh, M. Ghorbani-Asl, G. Hlawacek, A.V. Krasheninnikov, Supported two-dimensional materials under ion irradiation: the substrate governs defect production. ACS Appl. Mater. Interfaces **10**(36), 30827 (2018)
81. Q. Qian, L. Peng, N. Perea-Lopez, K. Fujisawa, K. Zhang, X. Zhang, T.H. Choudhury, J.M. Redwing, M. Terrones, X. Ma, Defect creation in WSe_2 with a microsecond photoluminescence lifetime by focused ion beam irradiation. Nanoscale **12**(3), 2047 (2020)
82. J.P. Thiruraman, K. Fujisawa, G. Danda, P.M. Das, T. Zhang, A. Bolotsky, N. Perea-López, A. Nicolaï, P. Senet, M. Terrones, Angstrom-size defect creation and ionic transport through pores in single-layer MoS_2. Nano Lett. **18**(3), 1651 (2018)
83. K. Parto, S.I. Azzam, K. Banerjee, G. Moody, Defect and strain engineering of monolayer WSe2 enables site-controlled single-photon emission up to 150 K. Nat. Commun. **12**(1), 1 (2021)
84. H. Nan, R. Zhou, X. Gu, S. Xiao, K.K. Ostrikov, Recent advances in plasma modification of 2D transition metal dichalcogenides. Nanoscale **11**(41), 19202 (2019)
85 Z. Lin, G.H. Waller, Y. Liu, M. Liu, C. Wong, 3D Nitrogen-doped graphene prepared by pyrolysis of graphene oxide with polypyrrole for electrocatalysis of oxygen reduction reaction. Nano Energy **2**(2), 241 (2013)
86. Y. Zhang, H. Tao, T. Li, S. Du, J. Li, Y. Zhang, X. Yang, Vertically oxygen-incorporated MoS_2 nanosheets coated on carbon fibers for sodium-ion batteries. ACS Appl. Mater. Interfaces. **10**(41), 35206 (2018)
87. X. Wei, Z. Yu, F. Hu, Y. Cheng, L. Yu, X. Wang, M. Xiao, J. Wang, X. Wang, Y. Shi, Mo-O bond doping and related-defect assisted enhancement of photoluminescence in monolayer MoS_2. AIP Adv. **4**(12), 123004 (2014)
88 M. Ghorbani-Asl, S. Kretschmer, D.E. Spearot, A.V. Krasheninnikov, Two-dimensional MoS_2 under ion irradiation: from controlled defect production to electronic structure engineering. 2D Mater. **4**(2), 025078 (2017)
89. J. Shim, A. Oh, D.H. Kang, S. Oh, S.K. Jang, J. Jeon, M.H. Jeon, M. Kim, C. Choi, J. Lee, High-performance 2D rhenium disulfide (ReS_2) transistors and photodetectors by oxygen plasma treatment. Adv. Mater. **28**(32), 6985 (2016)
90. P.K. Chow, R.B. Jacobs-Gedrim, J. Gao, T.-M. Lu, B. Yu, H. Terrones, N. Koratkar, Defect-induced photoluminescence in monolayer semiconducting transition metal dichalcogenides. ACS Nano **9**(2), 1520 (2015)
91. P. Lin, J. Shen, X. Yu, Q. Liu, D. Li, H. Tang, Construction of Ti_3C_2 MXene/O-doped g-C_3N_4 2D–2D Schottky-junction for enhanced photocatalytic hydrogen evolution. Ceram. Int. **45**(18), 24656 (2019)
92. S. Yang, Y. Chen, C. Jiang, Strain engineering of two-dimensional materials: methods, properties, and applications. InfoMat. **3**(4), 397 (2021)
93. C. Zhu, G. Wang, B. Liu, X. Marie, X. Qiao, X. Zhang, X. Wu, H. Fan, P. Tan, T. Amand, Strain tuning of optical emission energy and polarization in monolayer and bilayer MoS_2. Phys. Rev. B. **88**(12), 121301 (2013)

94. D. Vella, J. Bico, A. Boudaoud, B. Roman, P.M. Reis, The macroscopic delamination of thin films from elastic substrates. Proc. Natl. Acad. Sci. USA **106**(27), 10901 (2009)
95. C. Martella, C. Mennucci, E. Cinquanta, A. Lamperti, E. Cappelluti, F. Buatier de Mongeot, A. Molle, Anisotropic MoS_2 nanosheets grown on self-organized nanopatterned substrates. Adv. Mater. **29**(19), 1605785 (2017)
96. A.V. Tyurnina, D.A. Bandurin, E. Khestanova, V.G. Kravets, M. Koperski, F. Guinea, A.N. Grigorenko, A.K. Geim, I.V. Grigorieva, Strained bubbles in van der Waals heterostructures as local emitters of photoluminescence with adjustable wavelength. ACS Photon. **6**(2), 516 (2019)
97. P. Ares, Y.B. Wang, C.R. Woods, J. Dougherty, L. Fumagalli, F. Guinea, B. Davidovitch, K.S. Novoselov, Van der Waals interaction affects wrinkle formation in two-dimensional materials. Proc. Natl. Acad. Sci. USA (2021). https://doi.org/10.1073/pnas.2025870118
98. J.-P. So, H.-R. Kim, H. Baek, K.-Y. Jeong, H.-C. Lee, W. Huh, Y.S. Kim, K. Watanabe, T. Taniguchi, J. Kim, Electrically driven strain-induced deterministic single-photon emitters in a van der Waals heterostructure. Sci. Adv. **7**(43), eabj3176 (2021)
99. D. Li, C. Wei, J. Song, X. Huang, F. Wang, K. Liu, W. Xiong, X. Hong, B. Cui, A. Feng, Anisotropic enhancement of second-harmonic generation in monolayer and bilayer MoS_2 by integrating with TiO_2 nanowires. Nano Lett. **19**(6), 4195 (2019)
100. J. Liang, J. Zhang, Z. Li, H. Hong, J. Wang, Z. Zhang, X. Zhou, R. Qiao, J. Xu, P. Gao, Monitoring local strain vector in atomic-layered $MoSe_2$ by second-harmonic generation. Nano Lett. **17**(12), 7539 (2017)
101. P.T.K. Loan, W. Zhang, C.T. Lin, K.H. Wei, L.J. Li, C.H. Chen, Graphene/MoS2 heterostructures for ultrasensitive detection of DNA hybridisation. Adv. Mater. **26**(28), 4838 (2014)
102. S. Zeng, S. Hu, J. Xia, T. Anderson, X.-Q. Dinh, X.-M. Meng, P. Coquet, K.-T. Yong, Graphene–MoS_2 hybrid nanostructures enhanced surface plasmon resonance biosensors. Sens. Actuators, B **207**, 801 (2015)
103. N. Rohaizad, C.C. Mayorga-Martinez, M. Fojtů, N.M. Latiff, M. Pumera, Two-dimensional materials in biomedical, biosensing and sensing applications. Chem. Soc. Rev. **50**(1), 619 (2021)
104. M. Nasir, M.H. Nawaz, U. Latif, M. Yaqub, A. Hayat, A. Rahim, An overview on enzyme-mimicking nanomaterials for use in electrochemical and optical assays. Microchim. Acta **184**(2), 323 (2017)
105. L. Cheng, C. Yuan, S. Shen, X. Yi, H. Gong, K. Yang, Z. Liu, Bottom-up synthesis of metal-ion-doped WS_2 nanoflakes for cancer theranostics. ACS Nano **9**(11), 11090 (2015)
106. J. Li, Z. Yang, Y. Zhang, S. Yu, Q. Xu, Q. Qu, X. Hu, Tin disulfide nanoflakes decorated with gold nanoparticles for direct electrochemistry of glucose oxidase and glucose biosensing. Microchim. Acta **179**(3), 265 (2012)
107. Y. Jin, J. Wang, H. Ke, S. Wang, Z. Dai, Graphene oxide modified PLA microcapsules containing gold nanoparticles for ultrasonic/CT bimodal imaging guided photothermal tumor therapy. Biomaterials **34**(20), 4794 (2013)
108. S. Wang, X. Li, Y. Chen, X. Cai, H. Yao, W. Gao, Y. Zheng, X. An, J. Shi, H. Chen, A facile one-pot synthesis of a two-dimensional MoS_2/Bi_2S_3 composite theranostic nanosystem for multi-modality tumor imaging and therapy. Adv. Mater. **27**(17), 2775 (2015)
109. H. Lin, S. Gao, C. Dai, Y. Chen, J. Shi, A two-dimensional biodegradable niobium carbide (MXene) for photothermal tumor eradication in NIR-I and NIR-II biowindows. J. Am. Chem. Soc. **139**(45), 16235 (2017)
110. X. Dong, W. Yin, X. Zhang, S. Zhu, X. He, J. Yu, J. Xie, Z. Guo, L. Yan, X. Liu, Intelligent MoS_2 nanotheranostic for targeted and enzyme-/pH-/NIR-responsive drug delivery to overcome cancer chemotherapy resistance guided by PET imaging. ACS Appl. Mater. Interfaces **10**(4), 4271 (2018)
111. S. Shi, C. Xu, K. Yang, S. Goel, H.F. Valdovinos, H. Luo, E.B. Ehlerding, C.G. England, L. Cheng, F. Chen, Chelator-free radiolabeling of nanographene: breaking the stereotype of chelation. Angew. Chem. Int. Ed. **56**(11), 2889 (2017)
112. T. Liu, S. Shi, C. Liang, S. Shen, L. Cheng, C. Wang, X. Song, S. Goel, T.E. Barnhart, W. Cai, Iron oxide decorated MoS_2 nanosheets with double PEGylation for chelator-free radiolabeling and multimodal imaging guided photothermal therapy. ACS Nano **9**(1), 950 (2015)
113. L. Cheng, S. Shen, S. Shi, Y. Yi, X. Wang, G. Song, K. Yang, G. Liu, T.E. Barnhart, W. Cai, $FeSe_2$-decorated Bi_2Se_3 nanosheets fabricated via cation exchange for chelator-free ^{64}Cu-labeling and multimodal image-guided photothermal-radiation therapy. Adv. Funct. Mater. **26**(13), 2185 (2016)
114. K. Yang, L. Feng, X. Shi, Z. Liu, Nano-graphene in biomedicine: theranostic applications. Chem. Soc. Rev. **42**(2), 530 (2013)
115. C. Dai, H. Lin, G. Xu, Z. Liu, R. Wu, Y. Chen, Biocompatible 2D titanium carbide (MXenes) composite nanosheets for pH-responsive MRI-guided tumor hyperthermia. Chem. Mater. **29**(20), 8637 (2017)
116. D. Yang, G. Yang, P. Yang, R. Lv, S. Gai, C. Li, F. He, J. Lin, Assembly of Au plasmonic photothermal agent and iron oxide nanoparticles on ultrathin black phosphorus for targeted photothermal and photodynamic cancer therapy. Adv. Funct. Mater. **27**(18), 1700371 (2017)
117. H. Huang, W. Feng, Y. Chen, Two-dimensional biomaterials: material science, biological effect and biomedical engineering applications. Chem. Soc. Rev. (2021).
118. M.K. Tsang, Y.T. Wong, J. Hao, Cutting-edge nanomaterials for advanced multimodal bioimaging applications. Small Methods. **2**(1), 1700265 (2018)

119. S. Huang, R. Pandey, I. Barman, J. Kong, M. Dresselhaus, Raman enhancement of blood constituent proteins using graphene. ACS Photon. **5**(8), 2978 (2018)
120. Z. Wang, J. Ye, K. Zhang, L. Ding, T. Granzier-Nakajima, J. C. Ranasinghe, Y. Xue, S. Sharma, I. Biase, M. Terrones, S.H. Choi, C. Ran, R.E. Tanzi, S. Huang, C. Zhang, S. Huang, Rapid biomarker screening of Alzheimer's disease by interpretable machine learning and graphene-assisted Raman spectroscopy. *bioRxiv.* (2021).
121. Z. Liu, H. Chen, Y. Jia, W. Zhang, H. Zhao, W. Fan, W. Zhang, H. Zhong, Y. Ni, Z. Guo, A two-dimensional fingerprint nanoprobe based on black phosphorus for bio-SERS analysis and chemo-photothermal therapy. Nanoscale **10**(39), 18795 (2018)
122. C.W. Freudiger, W. Min, B.G. Saar, S. Lu, G.R. Holtom, C. He, J.C. Tsai, J.X. Kang, X.S. Xie, Label-free biomedical imaging with high sensitivity by stimulated Raman scattering microscopy. Science **322**(5909), 1857 (2008)
123. L. Mostaço-Guidolin, N.L. Rosin, T.-L. Hackett, Imaging collagen in scar tissue: developments in second harmonic generation microscopy for biomedical applications. Int. J. Mol. Sci. **18**(8), 1772 (2017)
124. J. Adur, H.F. Carvalho, C.L. Cesar, V.H. Casco, Nonlinear microscopy techniques: principles and biomedical applications, in *Microscopy and Analysis*, (IntechOpen, City, 2016).
125. C. Krafft, B. Dietzek, J. Popp, M. Schmitt, Raman and coherent anti-Stokes Raman scattering microspectroscopy for biomedical applications. J. Biomed. Opt. **17**(4), 040801 (2012)
126. T. Gottschall, T. Meyer, M. Baumgartl, C. Jauregui, M. Schmitt, J. Popp, J. Limpert, A. Tünnermann, Fiber-based light sources for biomedical applications of coherent anti-Stokes Raman scattering microscopy. Laser Photon. Rev. **9**(5), 435 (2015)
127. D. Wang, J.F.C. Loo, J. Chen, Y. Yam, S.-C. Chen, H. He, S.K. Kong, H.P. Ho, Recent advances in surface plasmon resonance imaging sensors. Sensors **19**(6), 1266 (2019)
128 E.P. Nguyen, C.C.C. Silva, A. Merkoçi, Recent advancement in biomedical applications on the surface of two-dimensional materials: from biosensing to tissue engineering. Nanoscale **12**(37), 19043 (2020)
129. T. Hu, X. Mei, Y. Wang, X. Weng, R. Liang, M. Wei, Two-dimensional nanomaterials: fascinating materials in biomedical field. Sci. Bull. **64**(22), 1707 (2019)
130. H. Shen, L. Zhang, M. Liu, Z. Zhang, Biomedical applications of graphene. Theranostics **2**(3), 283 (2012)
131. C. Huang, X. Zhang, Y. Li, X. Yang, Hyaluronic acid and graphene oxide loaded silicon contact lens for corneal epithelial healing. J. Biomater. Sci. Polym. Ed. **32**(3), 372 (2021)
132. Y. Yun, H. Wu, J. Gao, W. Dai, L. Deng, O. Lv, Y. Kong, Facile synthesis of Ca^{2+}-crosslinked sodium alginate/graphene oxide hybrids as electro-and pH-responsive drug carrier. Mater. Sci. Eng. C **108**, 110380 (2020)
133. J. Jampilek, K. Kralova, Advances in drug delivery nanosystems using graphene-based materials and carbon nanotubes. Materials **14**(5), 1059 (2021)
134 M. Mirza-Aghayan, M. Heidarian, M. Mohammadi, R. Boukherroub, Synthesis and characterization of a novel multifunctionalized reduced graphene oxide as a pH-sensitive drug delivery material and a photothermal candidate. Appl. Surf. Sci. **583**, 152568 (2022)
135. S. Xiong, J. Luo, Q. Wang, Z. Li, J. Li, Q. Liu, L. Gao, S. Fang, Y. Li, H. Pan, Targeted graphene oxide for drug delivery as a therapeutic nanoplatform against Parkinson's disease. Biomater. Sci. **9**(5), 1705 (2021)
136. M.H. Shin, E.Y. Park, S. Han, H.S. Jung, D.H. Keum, G.H. Lee, T. Kim, C. Kim, K.S. Kim, S.H. Yun, Multimodal cancer theranosis using hyaluronate-conjugated molybdenum disulfide. Adv. Healthc. Mater. **8**(1), 1801036 (2019)
137. L. Chen, J. Xu, Y. Wang, R. Huang, Ultra-small MoS_2 nanodots-incorporated mesoporous silica nanospheres for pH-sensitive drug delivery and CT imaging. J. Mater. Sci. Technol. **63**, 91 (2021)
138. U. Uthappa, O. Arvind, G. Sriram, D. Losic, M. Kigga, M.D. Kurkuri, Nanodiamonds and their surface modification strategies for drug delivery applications. J. Drug Deliv. Sci. Technol. **60**, 101993 (2020)
139. F. Yin, B. Gu, Y. Lin, N. Panwar, S.C. Tjin, J. Qu, S.P. Lau, K.-T. Yong, Functionalized 2D nanomaterials for gene delivery applications. Coord. Chem. Rev. **347**, 77 (2017)
140. S. Chung, R.A. Revia, M. Zhang, Graphene quantum dots and their applications in bioimaging, biosensing, and therapy. Adv. Mater. **33**(22), 1904362 (2021)
141. H. Zhao, R. Ding, X. Zhao, Y. Li, L. Qu, H. Pei, L. Yildirimer, Z. Wu, W. Zhang, Graphene-based nanomaterials for drug and/or gene delivery, bioimaging, and tissue engineering. Drug Discov. Today **22**(9), 1302 (2017)
142. R.T. Bartus, M.S. Weinberg, R.J. Samulski, Parkinson's disease gene therapy: success by design meets failure by efficacy. Mol. Ther. **22**(3), 487 (2014)
143. E. Keles, Y. Song, D. Du, W.-J. Dong, Y. Lin, Recent progress in nanomaterials for gene delivery applications. Biomater. Sci. **4**(9), 1291 (2016)
144. S.M. Elbashir, J. Harborth, W. Lendeckel, A. Yalcin, K. Weber, T. Tuschl, Duplexes of 21-nucleotide RNAs mediate RNA interference in cultured mammalian cells. Nature **411**(6836), 494 (2001)
145. L. Feng, X. Yang, X. Shi, X. Tan, R. Peng, J. Wang, Z. Liu, Polyethylene glycol and polyethylenimine dual-functionalized nano-graphene oxide for photothermally enhanced gene delivery. Small **9**(11), 1989 (2013)
146. N.D.Q. Chau, G. Reina, J. Raya, I.A. Vacchi, C. Ménard-Moyon, Y. Nishina, A. Bianco, Elucidation of siRNA

complexation efficiency by graphene oxide and reduced graphene oxide. Carbon **122**, 643 (2017)

147. F. Yin, K. Hu, Y. Chen, M. Yu, D. Wang, Q. Wang, K.-T. Yong, F. Lu, Y. Liang, Z. Li, SiRNA delivery with PEGylated graphene oxide nanosheets for combined photothermal and genetherapy for pancreatic cancer. Theranostics **7**(5), 1133 (2017)
148. F. Yin, K. Hu, S. Chen, D. Wang, J. Zhang, M. Xie, D. Yang, M. Qiu, H. Zhang, Z. Li, Black phosphorus quantum dot based novel siRNA delivery systems in human pluripotent teratoma PA-1 cells. J. Mater. Chem. B **5**(27), 5433 (2017)
149. T. Jiang, W. Sun, Q. Zhu, N.A. Burns, S.A. Khan, R. Mo, Z. Gu, Furin-mediated sequential delivery of anticancer cytokine and small-molecule drug shuttled by graphene. Adv. Mater. **27**(6), 1021 (2015)
150. S. Su, J. Wang, J. Wei, R. Martínez-Zaguilán, J. Qiu, S. Wang, Efficient photothermal therapy of brain cancer through porphyrin functionalized graphene oxide. New J. Chem. **39**(7), 5743 (2015)
151 H. Kim, D. Lee, J. Kim, T. Kim, W.J. Kim, Photothermally triggered cytosolic drug delivery via endosome disruption using a functionalized reduced graphene oxide. ACS Nano **7**(8), 6735 (2013)
152. M. Li, X. Yang, J. Ren, K. Qu, X. Qu, Using graphene oxide high near-infrared absorbance for photothermal treatment of Alzheimer's disease. Adv. Mater. **24**(13), 1722 (2012)
153. X. Zeng, M. Luo, G. Liu, X. Wang, W. Tao, Y. Lin, X. Ji, L. Nie, L. Mei, Polydopamine-modified black phosphorous nanocapsule with enhanced stability and photothermal performance for tumor multimodal treatments. Adv. Sci. **5**(10), 1800510 (2018)
154. Y.Y. Illarionov, M. Waltl, G. Rzepa, J.-S. Kim, S. Kim, A. Dodabalapur, D. Akinwande, T. Grasser, Long-term stability and reliability of black phosphorus field-effect transistors. ACS Nano **10**(10), 9543 (2016)
155. B. Wan, B. Yang, Y. Wang, J. Zhang, Z. Zeng, Z. Liu, W. Wang, Enhanced stability of black phosphorus field-effect transistors with SiO_2 passivation. Nanotechnology **26**(43), 435702 (2015)
156. A. Avsar, I.J. Vera-Marun, J.Y. Tan, K. Watanabe, T. Taniguchi, A.H. Castro Neto, B. Ozyilmaz, Air-stable transport in graphene-contacted, fully encapsulated ultrathin black phosphorus-based field-effect transistors. ACS Nano **9**(4), 4138 (2015)
157. Y. Zhao, H. Wang, H. Huang, Q. Xiao, Y. Xu, Z. Guo, H. Xie, J. Shao, Z. Sun, W. Han, Surface coordination of black phosphorus for robust air and water stability. Angew. Chem. **128**(16), 5087 (2016)
158. B. Yang, B. Wan, Q. Zhou, Y. Wang, W. Hu, W. Lv, Q. Chen, Z. Zeng, F. Wen, J. Xiang, Te-doped black phosphorus field-effect transistors. Adv. Mater. **28**(42), 9408 (2016)
159. X. Zhu, T. Zhang, D. Jiang, H. Duan, Z. Sun, M. Zhang, H. Jin, R. Guan, Y. Liu, M. Chen, Stabilizing black phosphorus nanosheets via edge-selective bonding of sacrificial C60 molecules. Nat. Commun. **9**(1), 1 (2018)
160. A.S. Dikkumbura, P. Hamal, M. Chen, D.A. Babayode, J.C. Ranasinghe, K. Lopata, L.H. Haber, Growth dynamics of colloidal silver-gold core–shell nanoparticles studied by in situ second harmonic generation and extinction spectroscopy. J. Phys. Chem. C **125**(46), 25615 (2021)
161. R.A. Khoury, J.C. Ranasinghe, A.S. Dikkumbura, P. Hamal, R.R. Kumal, T.E. Karam, H.T. Smith, L.H. Haber, Monitoring the seed-mediated growth of gold nanoparticles using in situ second harmonic generation and extinction spectroscopy. J. Phys. Chem. C **122**(42), 24400 (2018)
162. J.C. Ranasinghe, A.S. Dikkumbura, P. Hamal, M. Chen, R.A. Khoury, H.T. Smith, K. Lopata, L.H. Haber, Monitoring the growth dynamics of colloidal gold-silver core-shell nanoparticles using in situ second harmonic generation and extinction spectroscopy. J. Chem. Phys. **151**(22), 224701 (2019)
163. K. Wang, Q. Chen, W. Xue, S. Li, Z. Liu, Combined chemo-photothermal antitumor therapy using molybdenum disulfide modified with hyperbranched polyglycidyl. ACS Biomater. Sci. Eng. **3**(10), 2325 (2017)
164 S. GhorbanzadehSheish, R. Emadi, M. Ahmadian, S. Sadeghzade, F. Tavangarian, Fabrication and characterization of polyvinylpyrrolidone-eggshell membrane-reduced graphene oxide nanofibers for tissue engineering applications. Polymers **13**(6), 913 (2021)
165. R.V. Chernozem, K.N. Romanyuk, I. Grubova, P.V. Chernozem, M.A. Surmeneva, Y.R. Mukhortova, M. Wilhelm, T. Ludwig, S. Mathur, A.L. Kholkin, Enhanced piezoresponse and surface electric potential of hybrid biodegradable polyhydroxybutyrate scaffolds functionalized with reduced graphene oxide for tissue engineering. Nano Energy **89**, 106473 (2021)
166. C. Gardin, A. Piattelli, B. Zavan, Graphene in regenerative medicine: focus on stem cells and neuronal differentiation. Trends Biotechnol. **34**(6), 435 (2016)
167. G. Choe, S.-W. Kim, J. Park, J. Park, S. Kim, Y.S. Kim, Y. Ahn, D.-W. Jung, D.R. Williams, J.Y. Lee, Anti-oxidant activity reinforced reduced graphene oxide/alginate microgels: mesenchymal stem cell encapsulation and regeneration of infarcted hearts. Biomaterials **225**, 119513 (2019)
168. X. Liu, A.L. Miller, S. Park, M.N. George, B.E. Waletzki, H. Xu, A. Terzic, L. Lu, Two-dimensional black phosphorus and graphene oxide nanosheets synergistically enhance cell proliferation and osteogenesis on 3D printed scaffolds. ACS Appl. Mater. Interfaces **11**(26), 23558 (2019)
169. K. Huang, J. Wu, Z. Gu, Black phosphorus hydrogel scaffolds enhance bone regeneration via a sustained supply of calcium-free phosphorus. ACS Appl. Mater. Interfaces **11**(3), 2908 (2018)
170. Y. Wang, X. Hu, L. Zhang, C. Zhu, J. Wang, Y. Li, Y. Wang, C. Wang, Y. Zhang, Q. Yuan, Bioinspired extracellular vesicles

embedded with black phosphorus for molecular recognition-guided biomineralization. Nat. Commun. **10**(1), 1 (2019)

171. M. Annunziata, A. Oliva, M.A. Basile, M. Giordano, N. Mazzola, A. Rizzo, A. Lanza, L. Guida, The effects of titanium nitride-coating on the topographic and biological features of TPS implant surfaces. J. Dent. **39**(11), 720 (2011)
172. F. Veronesi, G. Giavaresi, M. Fini, G. Longo, C.A. Ioannidu, A.S. d'Abusco, F. Superti, G. Panzini, C. Misiano, A. Palattella, Osseointegration is improved by coating titanium implants with a nanostructured thin film with titanium carbide and titanium oxides clustered around graphitic carbon. Mater. Sci. Eng. C **70**, 264 (2017)
173. Y. Fu, J. Zhang, H. Lin, A. Mo, 2D titanium carbide (MXene) nanosheets and 1D hydroxyapatite nanowires into free standing nanocomposite membrane: In vitro and in vivo evaluations for bone regeneration. Mater. Sci. Eng. C **118**, 111367 (2021)
174. S. Wu, J. Wang, L. Jin, Y. Li, Z. Wang, Effects of polyacrylonitrile/MoS_2 composite nanofibers on the growth behavior of bone marrow mesenchymal stem cells. ACS Appl. Nano Mater. **1**(1), 337 (2017)
175. H. Nazari, A. Heirani-Tabasi, M.S. Alavijeh, Z.S. Jeshvaghani, E. Esmaeili, S. Hosseinzadeh, F. Mohabatpour, B. Taheri, S.H.A. Tafti, M. Soleimani, Nanofibrous composites reinforced by MoS_2 nanosheets as a conductive scaffold for cardiac tissue engineering. ChemistrySelect **4**(39), 11557 (2019)
176. S. Unal, N. Ekren, A.Z. Sengil, F.N. Oktar, S. Irmak, O. Oral, Y.M. Sahin, O. Kilic, S. Agathopoulos, O. Gunduz, Synthesis, characterization, and biological properties of composites of hydroxyapatite and hexagonal boron nitride. J. Biomed. Mater. Res. B. **106**(6), 2384 (2018)
177. K.R. Foster, R. Koprowski, J.D. Skufca, Machine learning, medical diagnosis, and biomedical engineering research-commentary. Biomed. Eng. Online. **13**(1), 1 (2014)
178. W. Luo, D. Phung, T. Tran, S. Gupta, S. Rana, C. Karmakar, A. Shilton, J. Yearwood, N. Dimitrova, T.B. Ho, Guidelines for developing and reporting machine learning predictive models in biomedical research: a multidisciplinary view. J. Med. Internet Res. **18**(12), e5870 (2016)
179. S. Berg, D. Kutra, T. Kroeger, C.N. Straehle, B.X. Kausler, C. Haubold, M. Schiegg, J. Ales, T. Beier, M. Rudy, Ilastik: interactive machine learning for (bio) image analysis. Nat. Methods **16**(12), 1226 (2019)
180. T. Jo, K. Nho, A.J. Saykin, Deep learning in Alzheimer's disease: diagnostic classification and prognostic prediction using neuroimaging data. Front. Aging Neurosci. **11**, 220 (2019)
181. S.A.A. Ismael, A. Mohammed, H. Hefny, An enhanced deep learning approach for brain cancer MRI images classification using residual networks. Artif. Intell. Med. **102**, 101779 (2020)
182. L. Sharma, G. Gupta, V. Jaiswal, Classification and development of tool for heart diseases (MRI images) using machine learning, in *2016 Fourth International Conference on Parallel, Distributed and Grid Computing* (*PDGC*), (IEEE, City, 2016), p. 219.
183. K. He, X. Zhang, S. Ren, J. Sun, Deep residual learning for image recognition, in *Proceedings of the IEEE Conference on Computer Vision and Pattern Recognition,* (City, 2016), pp. 770.
184. S. Naeem, A. Ali, S. Qadri, W. Khan Mashwani, N. Tairan, H. Shah, M. Fayaz, F. Jamal, C. Chesneau, S. Anam, Machine-Learning based hybrid-feature analysis for liver cancer classification using fused (MR and CT) images. Appl. Sci. **10**(9), 3134 (2020)
185. S.H. Kassania, P.H. Kassanib, M.J. Wesolowskic, K.A. Schneidera, R. Detersa, Automatic detection of coronavirus disease (COVID-19) in X-ray and CT images: a machine learning based approach. Biocybern. Biomed. Eng. **41**(3), 867 (2021)
186. M. Barstugan, U. Ozkaya, S. Ozturk, Coronavirus (covid-19) classification using ct images by machine learning methods. arXiv preprint arXiv:2003.09424. (2020)
187. J. Ye, Y. -T. Yeh, Y. Xue, Z. Wang, N. Zhang, H. Liu, K. Zhang, Z. Yu, A. Roder, N. P. Lopez, L. Organtini, W. Greene, S. Hafenstein, H. Lu, E. Ghedin, M. Terrones, S. Huang, S. Xiaolei Huang, Accurate virus identification with interpretable raman signatures by machine learning. Proc. Natl. Acad. Sci. U.S.A (2021)
188. S. Das, H. Pegu, K. K. Sahu, A. K. Nayak, S. Ramakrishna, D. Datta, S. Swayamjyoti, Machine learning in materials modeling—fundamentals and the opportunities in 2D materials, in *Synthesis, Modeling, and Characterization of 2D Materials, and Their Heterostructures* (Elsevier, City, 2020), p. 445
189 N.C. Frey, J. Wang, G.I. Vega Bellido, B. Anasori, Y. Gogotsi, V.B. Shenoy, Prediction of synthesis of 2D metal carbides and nitrides (MXenes) and their precursors with positive and unlabeled machine learning. ACS Nano **13**(3), 3031 (2019)
190. H. Tao, T. Wu, M. Aldeghi, T.C. Wu, A. Aspuru-Guzik, E. Kumacheva, Nanoparticle synthesis assisted by machine learning. Nat. Rev. Mater. **6**(8), 701 (2021)
191. W. Huyer, A. Neumaier, SNOBFIT–stable noisy optimization by branch and fit. ACM Trans. Math. Softw. **35**(2), 1 (2008)
192. S. Krishnadasan, R. Brown, A. Demello, J. Demello, Intelligent routes to the controlled synthesis of nanoparticles. Lab Chip **7**(11), 1434 (2007)
193. J. Li, J. Li, R. Liu, Y. Tu, Y. Li, J. Cheng, T. He, X. Zhu, Autonomous discovery of optically active chiral inorganic perovskite nanocrystals through an intelligent cloud lab. Nat. Commun. **11**(1), 1 (2020)
194. Y. Jia, X. Hou, Z. Wang, X. Hu, Machine learning boosts the design and discovery of nanomaterials. ACS Sustain. Chem. Eng. **9**(18), 6130 (2021)

195. B. Sun, M. Fernandez, A.S. Barnard, Machine learning for silver nanoparticle electron transfer property prediction. J. Chem. Inf. Model. **57**(10), 2413 (2017)
196. G.P. Neupane, L. Zhang, T. Yildirim, K. Zhou, B. Wang, Y. Tang, W. Ma, Y. Xue, Y. Lu, A prospective future towards bio/medical technology and bioelectronics based on 2D vdWs heterostructures. Nano Res. **13**(1), 1 (2020)
197. M.E. Marchwiany, M. Birowska, M. Popielski, J.A. Majewski, A.M. Jastrzębska, Surface-related features responsible for cytotoxic behavior of MXenes layered materials predicted with machine learning approach. Materials **13**(14), 3083 (2020)
198. Z. Yin, H. Ai, L. Zhang, G. Ren, Y. Wang, Q. Zhao, H. Liu, Predicting the cytotoxicity of chemicals using ensemble learning methods and molecular fingerprints. J. Appl. Toxicol. **39**(10), 1366 (2019)
199. H. Yin, Z. Sun, Z. Wang, D. Tang, C.H. Pang, X. Yu, A.S. Barnard, H. Zhao, Z. Yin, The data-intensive scientific revolution occurring where two-dimensional materials meet machine learning. Cell Rep. Phys. Sci. **2**(7), 100482 (2021)
200. A.V. Singh, M.H.D. Ansari, D. Rosenkranz, R.S. Maharjan, F.L. Kriegel, K. Gandhi, A. Kanase, R. Singh, P. Laux, A. Luch, Artificial intelligence and machine learning in computational nanotoxicology: unlocking and empowering nanomedicine. Adv. Healthc. Mater. **9**(17), 1901862 (2020)